Prakash Pandey

ACID SULFATE SOILS

Leaching of Cobalt, Lithium, Nickel and Zinc

Bachelor's Thesis
CENTRIA UNIVERSITY OF APPLIED SCIENCES
Environmental Chemistry and Technology
December 2019

ABSTRACT

Centria University of Applied Sciences	Date December 2019	Author Prakash Pandey
Degree programme Environmental Chemistry and Technology		
Name of thesis ACID SULFATE SOILS- Leaching of cobalt, lithium, nickel and zinc.		
Instructor Anton Boman		**Pages** 69
Supervisor Jana Holm		

The aim of this thesis work was to analyse the leachate for metals such as Cobalt, Nickel, Lithium, and Zinc through Atomic Absorption Spectrometry. Furthermore, the leaching results were compared with the background values to determine the loss of these metals from soil to water during oxidation and leaching. The thesis further describes the formation of acid sulfate soil, which corresponds to the geo-chemistry of metastable iron sulfide, elemental S, sulfate, and organic S and pyrite.

In the laboratory experiment, preparation of the soil samples for Atomic Absorption Spectrometry analysis is presented. The initial set up starts with incubation and involves several steps such as pH measurement, drying, centrifugation, filtration, and acidification. The theoretical approach details the acid sulfate soil with its worldwide distribution as well as the essential indicators such as vegetation, water, soil, and infrastructure. The redox chemistry for the formation of acid sulfate soils and necessary redox conditions are presented. Lastly, the environmental impacts on vegetation, aquatic habitats, and human beings, as well as the management of these soils, are presented.

The lab results and conclusions section present three different zones for AS soils which are oxidizing, transitional and reduction zone. The metals amount is highly presented in reduced zones but leaching of metals occurs excessively from oxidized zones. Among these metals, cobalt is highly leached with its maximum value of 80% while zinc is least leached with 0%.

Key words
Acid Sulphate Soil, Atomic Absorption Spectrometry, Leaching, Potential Acid Sulphate Soil, Redox Chemistry

CONCEPT DEFINITIONS

Conceptional Definitions

Brackish water	Brackish water is formed by the mixture of fresh water and marine water resulting dilution of salts and chlorides with of pH range 6-9. The brackish water contains suspended particles such as silt and sand with particle size of 1-200 microns. (Nesbitt 2007, 56.)
Metastable iron sulfide	It consists of either mackinawite and gregnite. (Boman, 2008.)
Waterlogged condition	The condition with excess of water in soil that prevents the exchange of oxygen with atmosphere. This is also called as saturated soil. During the water-logged condition available oxygen is used up by biological activities and cause oxygen deficiency. (Government of Western Australia, 2019.)
Post glacial isostatic land uplift	During the glacial period, land was covered with large sheets of ice which pushes the earth crust downward. As the ice stats melting, the earth deforms and starts rising which is referred as post glacial isostatic land uplift. (Steffen & Kaufmann 2005)
Hydrolysis	It is defined as the removal of chemical bonds of organic compound with the use of water to form new substances without causing its decomposition. Hydrolysis can be acidic or enzymatic depending upon the content of feedstock. (Katyal & Morrison 2007, 520.)

Abbreviations

AS Soil	Acid Sulfate Soil
PAS Soil	Potential Acid Sulfate Soil
AAS	Atomic Absorption Spectroscopy

Chemical Compounds

Jarosite	$KFe_3(SO_4)_2(OH)_6$
Schwertmannite	$Fe_8O_8(OH)_6SO_4$
Fe oxyhydroxides	$Fe(OH)_3$and FeOOH
Mackinawite	FeS
Greigite	$FeS_{1.34}$

ABSTRACT
CONCEPT DEFINITIONS
CONTENTS

FIGURES

PICTURES

TABLES

1 INTRODUCTION

The aim of this study was to analyse the amount of metals such as Co, Li, Ni and Zn leaching from AS soils to water and compare the leaching result with background value to know how much metals are leached during oxidation. The metals concentration (ICE-OES) of the soil samples already exist and can be used for background concentration. The experience gained from this thesis will also help to enhance professional competence. The thesis work further presents the brief history about the AS soils identification and the necessary conditions for its formation. The total area covered by AS soils globally in Southeast Asia, West Africa, Eastern Australia, Latin America and Europe is also presented. The focus is on AS soils in Finland which covers almost half of the soil in Europe.

There may be some possible limitations of this thesis work. The top-most limitation would be the gap between the thesis topic and prior studies. Therefore, it absorbs plenty of time in researching documents and developing ideas for contents. The thesis work only presents leaching of metals from AS soils to water and can be improved by adding few more lab experiments such as sulfate analysis, EC and titratable incubation acidity. The leaching results are not in accordance with the theoretical approach because of the presence of sand and clay in soil mixtures which makes the soil inhomogeneous. The last limitation would be the lack of adequate soil samples and with larger soil samples more precise results would be obtained.

Acid sulfate soils are the soils which are oxidized such that the pH of the soil is dropped to 4 or below. In other words, AS soils are the oxidation product of PAS soil which are the parent sediment and remain under AS soils. AS soils contain reduced sulfur compounds such as pyrite and metastable iron sulfides which can oxidize and produce sulfuric acid and cause several environmental hazards. AS soils can be identified by soil, vegetations, water and infrastructure. Vegetations such as cauliflower and rose plant with deficiency of magnesium and iron are illustrated under section indicators of AS soils. AS soils are capable of leaching metals to water and affect its quality as well as kill aquatic habit, flora and fauna. This scenario can be observed under sub-section water indicators. AS soils attack cement externally, causing cracks, expansion and loss of bondage between cement and gypsum.

.

Several reducing and oxidizing conditions of AS soils are presented in sulfur redox chemistry and general principles section. Reduction process occurs when oxygen is consumed by oxic bacteria in the

breakdown of organic matter to CO_2 and enhances bacterial sulfate reduction. Likewise, O_2 is the oxidizing agent in PAS soils and Fe^{+3} in AS soils. The process oxidation in PAS soils and in AS soils is further presented with several chemical equations. AS soils are responsible for leaching several metals such as aluminum, cobalt, nickel, zinc, cadmium, manganese, iron and chromium to water sources. These metals can mobilize crops and enter the human body causing diseases such as Alzheimer and Parkinsons disease. The experimental results from metal mobilized in timothy plant and oat grains is presented in this thesis. The formation of AS soils can be managed by using control sub-surface drainage and control sub- surface irrigation technology.

For the laboratory setup, soil samples were sprayed with water, and the incubation pH was measured. Then the procedure followed by drying, centrifugation, filtration and acidification and the AAS experiment was performed at Centria UAS. The results show that three different zones are observed in AS soils which are oxidized, transitional and reduced zone. Metals are excessively leached from oxidized zone and least from reduced zone. Cobalt is excessively leached with its maximum value of 80% while zinc is least leached with 0%.

2 THEORETICAL BACKGROUND

This section includes various basic aspects of AS soil such as history, the definition of AS soil, and formation. The worldwide distribution of acid sulfate soil is further presented. The indicators for the identification of acid sulfate soil such as soil color, vegetation, water, and infrastructure are briefly discussed.

2.1 History

The AS soil was first recognized in 18th century by Carl Linnaeus in the Netherland and was named as 'Argilla Vitrio' which means soil with sulfuric acid (Dent & Pons 1995, 263-265). AS soils have been identified in South East Asia, East and West Africa, South and Central Africa, the United States and Australia. In 1972 AS soils were internationally discussed in the Netherland and since then it has been an essential topic for research in various parts of the world, especially in Finland, Sweden and Australia. Artificial and natural drainage plays a significant role in the production of AS soil in coastal areas of Finland while isostatic land uplift the sediments above the sea level. (Uusi-Kämppä, Keskinen, Heikkinen, Guagliardi, & Nuutinen 2019.)

About 8000 years ago, the conditions became more favourable for sulfate reduction where sulfate-reducing bacteria converted the plant residues and seawater sulfate of Baltic sea (also known as Litorina sea) into sulfides. These sulfides are not harmful in the absence of oxygen but result in the production of sulfuric acid in the presence of oxygen, which further decreases the pH level of soils from 6-7 to 4 or less. Consequently, this gives rise in the concentration of metals such as Al, Co, Li, Ni and Zn due to the dissolution of minerals. These metals can be leached to the water sources or uptaken by plants. (Uusi-Kämppä et al. 2019.)

In early 20 century acid sulfate soil were first recorded in Finland during agrogeological soil mappings in Ostrobothnia by Aarnio (Arnio 1928, 80). In 1970 all the fish were killed in river Kyrönjöki due tothe presence of acid sulfate soil (Björklund & Åström 1995). About half of the soil is situated in Ostrobothnia (Western Finland), which is the main reason for the toxicity in coastal areas of the Gulf of Bothnia. It is a fact that most of the metals leached from acid sulfate soil are higher than the entire Finnish industries. (Sundström, Åström, & Österholm 2002.)

2.2 ACID SULFATE SOILS

Acid sulfate soils are generally defined as soils, sediments (incl. glacial till) and organic materials (e.g. peat) containing hypersulfidic material in such quantities that the soil pH has dropped, or may drop, below 4 as a result of sulfide oxidation and the formation of sulfuric acid. Added to the Finnish-Swedish definition is that for organic soil materials (e.g. peat and gyttja) the pH needs to drop below 3. The reason for this is to be able to distinguish between acidity formed from sulfide oxidation and organic acids (cf. Hadzic et al. 2014). Acid sulfate soils are further divided into active (or actual), if sulfide oxidation has been initiated, and potential, if sulfide oxidation has not yet started. (Boman, Becher, Mattbäck, Sohlenius, Auri, Öhrling, Liwata-Kenttälä, & Edén 2019.)

AS soils are exposed to the environment either by post-glacial isostatic land uplift or by anthropogenic activities such as natural and artificial drainage, and ditching resulting in the formation of sulfuric acid. (Nordmyr et al 2006, 261-262; Boman 2008, 1-2.) The climatic situation such as drought further deepens the oxygen level in the ground resulting in acid sulfate soil (Virtanen, Simojoki, Rita, Toivonen, Hartikainen, & Yli-Halla 2014, 336-348). Their black (as shown in PICTURE 1) appearance represents the potential acid sulfate soil due to the presence of metastable iron sulfide. Likewise, they consist of 1% dry weight of iron sulfide, iron pyrite (FeS_2) and 95 % of total sulfur. They are generally fine-grained containing clay and silt particles. Also, sand can be presented in AS soils. (Boman et al 2008,1-2.) Along with a massive number of pyrite, potential acid sulfate soil consists of other sulfides such as greigite and mackinawite (Karimian, Johnston, & Burton 2018, 804). In picture 1 the symbol j represents jarosite, se for sulfides, qm for silica and pedogenic. The oxidized and unoxidized boundary occurs between Bsej2 and Cse around 80 cm

PICTURE 1. A complete AS soil profile (adapted from Wessel, Fiola, & Rabenhorst 2017, 261)

Another condition for occurrence of AS soil is neutralization soil capacity by exchanging calcium carbonate, exchangeable cations and weatherable silica minerals is much lower than potential acidity (Toivonen, Österholm, & Fröjdö 2013). This is the condition for acidification of soil with a pH value lower than 4. Three different layers with varying pH value are presented by the Figure 2 representing acidic layer, transition zone and parent sediment or potential acid sulphate layer. The acidic zone consists of oxidizable sulfur compounds with 3.5 pH value and give rise to pH by 0.5 when incubated at room temperature under moist condition with a time period of 8 weeks. In between the top and bottom layer, lies transition zone where the pH turns from acidic to neutral. (Boman et al. 2008, 1-4.) AS soil can be fine grained (<63 μm) or coarse grained (>63 μm). The acidity caused by fine grain is usually higher (10-100 times) than coarse grained. (Mattbäck et al. 2017.) The Figure 1 soil includes plow layer (0-40 cm from the surface), acidic horizon, transition zone and parent sediment (potential acid sulfate soil).

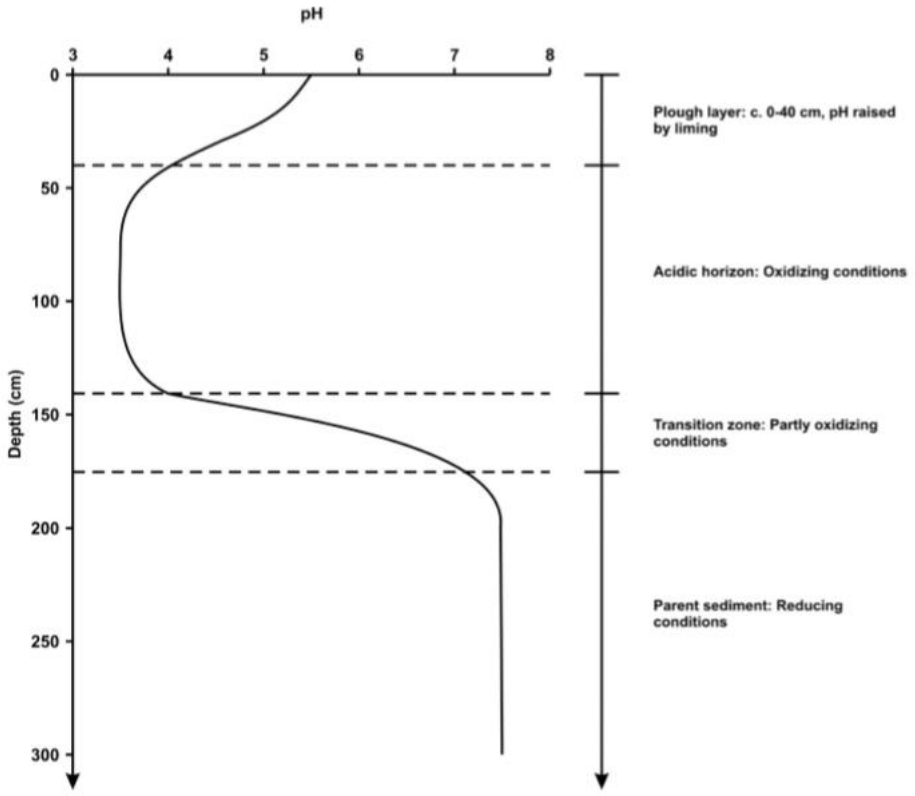

FIGURE 1. Variation of pH value with the depth of the) (adapted from Boman 2008)

2.3 Distribution of acid sulphate soil

The acid soil covers the area of 17 million ha or 170,000 km^2 worldwide and is located on the low coastal lands of Southeast Asia, West Africa, Eastern Australia, Latin America, and Europe and their worldwide share can be observed from Table 1(Adriesse, Van Mensvoort, 2006, 14-19). Most of these regions consist of high temperature, protected mangroves, and marches with a large amount of tidal exchange and facilitate pyrite accumulation ([Klu 2017, 3]). Likewise, in Finland, it occupies an area of 380 km^2 (Purokoski 1959) to 3360 km^2 (Palko 1994), which accounts for half of the soil in Europe. Acid Sulphate soil is situated at an altitude of 0-100 m above the sea level and are located mostly in Ostrobothnia, especially in Vaasa, but the highest concentration per hectar of sulfur is found in Oulu (Yli-Halla, Puustinen & Koskiaho 1999, 62-67). It has been found that the acid soil near river area has high load of acidity, Al, Tl, rare earth metals, alkali and alkaline earth metals (Li, Be, Na, Mg, K, Ca, Sr),transition metals (Mn, Co, Ni, Cu, Zn, Cd) and nonmetals (B, Si, S, Cl). The elements such as Ba, Ti, V, Cr, Fe, Mo, Pb, As and Sb are not found in these streams. (Österholm, & Åström 2002, 1210.)

TABLE 1. Worldwide distribution of Acid sulfate and potential Acid sulfate soil, the most is in Asia while the least in North America (adapted Adriesse et al 2009)

Continents	AS and PAS soils distribution in million ha
Africa	4,5
Asia	6,5
Latin America	3
Europe	0,235
Australia	3
North America	0,1
Total	17,335

2.4 Indicators for AS soil

The acid sulphate soil can be identified by several indications such as from the colors of soil and water. Different deficiencies can be observed in vegetations such rose and cauliflower in the presence of acidic soil. Likewise, effect on infrastructure such as corrosion appears due to acid soil.

2.4.1 Soil indicators

Undisturbed AS soils are usually wet with its pores filled with water (saturated soil) having gley or greenish in appearance. Presence of unpleasant odor like that of rotten egg can be felt which indicates the presence of H_2S gas due to the decomposition of sulfur and organic matter. The sulfidic material could be preserved in anaerobic soil condition. In contrast, disturbed soils are quite dry and consists of cracking on the surface. These kinds of soil are not distributed equally due to their shrinking nature and absence of water. The soil has yellow mottle (spots, blotches or steaks) which represent mineral jarosite as shown in Picture 2 or orange mottle which represent iron oxide. The soil has a light load-bearing capacity and can shrink due to excess load of construction activities. (Queensland Government 2013.)

PICTURE 2. Jarosite, a type of mineral available in acidic soil (adapted from Queensland government et al. 2013)

2.4.2 Vegetation indicators

The acidic soil causes deficiency of calcium and phosphorous in plants as well as increases toxic levels of manganese and aluminum. The deficiencies of magnesium in cauliflower and iron in rose plant are represented in Picture 3 and 4. Magnesium is an important mineral which helps in photosynthesis and pants growth. Acidic soils are one of the reasons for magnesium deficiency causing yellowing of leaves from outer leaves to middle as shown in Picture 3. The veins of the leaves remain white, stiff and fall off prematurely. There are several other plant species which grow in acidic environmental condition such as mangrove trees which grow in anaerobic soil conditions and supplies organic matter for the formation of acid sulfate soil in the coastal region in Australia. Similarly, marine couch or salt couch or salt grass, melaleuca species or ti-trees or paper barks, casuarina and allocasuarina species or she-oaks, phragmites austrails and water lilies are common in soil with low pH. (Queensland Government et al. 2016.)

PICTURE 3. Magnesium deficiency in cauliflower (adapted from government of Western Australia et al. 2014)

Iron helps to balance the plant nutrients and prevent from diseases. The scarcity of iron in soil causes yellowing of leaves (chlorosis) while the main veins of leaves remains green as shown in Picture 4. The alkaline or acidic soils locks up the iron in the soil and prevents its promotion to plants leaves. The iron deficiency occurs when the concentration of iron is less than 2mg/kg. In contrast, iron in rose plants helps to create chlorophyll, activate other enzymes which further activates nitrogen used by bush and keeps the plant in dark green color. The iron deficiency can be prevented by using spray with good amount of iron as a temporary measure, fertilizers such as ammonium sulfate and ammonium chloride for soils with high pH. Similarly, organic manure further helps to lower the soil pH. (Datta 2019)

PICTURE 4. Consequence of excessive use of mineral fertilizers in rose plant, leading to the deficiency of iron (adapted from Government of Western Australia et al. 2014)

2.4.3 Water indicator

Metals are leached from acid sulfate soil to water sources and degrade its quality. Soil with acid potential extracts the soil minerals such as aluminum. Low pH water and high aluminum facilitate flocculation and therefore suspended soil particles can be observed on the surface of the water. Finally, the suspended particles settle down, making the water clear or blue-green as shown in Picture 5. This incident occurred in Kyrönjöki river where almost all fish were killed, and water appeared clear (National Board of Waters 1973, 101). Likewise, reduced Fe^{2+} from acid sulfate soil form orange layer over the liquid when further oxidized in water. This unpleasant orange layer consists of an oily film of iron loving bacteria that remains stable even when it is disturbed. (Queensland Government, 2013.)

PICTURE 5. Blue green water indicating the solubility of aluminum in water through acidification nature of soil (adapted from Government of Western Australia et al. 2015, 3)

2.4.4 Infrastructure

Sulfate produced by AS soils attack concrete and leads to infrastructure failure. The sulfate attack can be external or internal. In the external sulfate attack (from AS soils), the water containing dissolved sulfate diffuses into cement, causes cracking, expansion, and loss of bondage between cement and gypsum, which results in loss of concrete strength. (Prasad, Jain & Ahuja 2006, 259-260.) While the internal sulfate attack refers to sulfur contamination during initial mixing process (Understanding cement 2005). Acidic water causes corrosion in concrete and steel. This phenomenon is common at the base of the bridge and canal walls. Likewise, cracks may be found on asphalt, and the area of land might sink unevenly, causing damage to infrastructure. The corrosion caused by AS soils to buildings can be observed from Picture 6. (Queensland Government et al. 2013.)

PICTURE 6. The corrosion caused by acid sulphate soil on a building (adapted from Queensland Government et al. 2013)

3 SULFUR REDOX CHEMISTRY AND GENERAL PRINCIPLES

This section provides a basic understanding of the chemical behavior and reactions for the formation of acid sulfate soil. The overall mechanism for the reducing and oxidizing conditions for acid sulfate soil is presented, and it is applicable for any acid sulfate soil. Likewise, the oxidation pattern for Finnish acid sulphate soil and potential acid sulphate soil is further presented in detail.

3.1 Reducing conditions

The reduction process is triggered by the sulfate-reducing bacteria when the oxygen is consumed by oxic bacteria during the breakdown of organic matter to carbon dioxide (CO_2) and facilitate anoxic conditions for bacterial sulphate reduction (Berner 1984). The reduction process is presented in equation 1, where CH_2O represents the organic matter (Boman, Fröjdö, Backlund, & Åström 2010, 1269). H_2S in the reactions (2 and 3) results in the formation of metastable iron sulfide (mackinawite) when H_2S reacts with iron (Price & Shieh 1979; Böttcher, Smock, & Cypionka 1998). The two different mechanisms for the formation of Fe are represented by equation 2 and 3 (Ricard 1995).

$$2CH_2O + SO_4^{2-} \rightarrow H_2S + 2HCO_3^- \quad (1)$$

$$Fe^{2+} + H_2S^- \rightarrow FeS + 2H^+ \quad (2)$$

$$Fe^{2+} + HS^- \rightarrow Fe(HS)_2 \rightarrow FeS + H_2S \quad (3)$$

Equation 2 is named as nanoparticulate mackinawite (Wolthers, Van der Gaast, & Rickard 2003) and consists of FeS(can be makinawite or greigite) in the ratio of 1:1(Ricard et al 2006) while the equation 3 is called a Bisulphide pathway. In the first step ofc the reaction in equation 3, intermediate complex ($Fe(HS)_2$) is formed which further condensates to give mackinawite (FeS) (Boman et al. 2008, 72). The Reaction pathway depends on the pH as well as total dissolved S (Ricard et al 1995). Therefore, in the given condition, when sulphide $< 10^{-3}$ M of total dissolved sulphide and pH < 8, equation 2 is dominated.

In contrast, if sulphide $\geq 10^{-3}$ M of total dissolved sulphide and pH > 7, reaction 3 is evolved (Ricard et al 1995).

The reactions mechanism for the formation of Pyrite is stated in equation 4 (Ricard 1997; Ricard & Luther 1997) and 5 (Ricard et al 1975; Luther 1991).

$$FeS + H_2S \rightarrow FeS_2 + H_2 \quad (4)$$

$$FeS + Sn^{2-} \rightarrow FeS_2 + S_{n-1}^{2-} \quad (5)$$

The reactions as presented in equation 4 and 5 are also called H_2S pathway (Ricard et al 1997; Ricard & Luther et al 1997) and polysulphide pathway (Ricard et al 1975; Luther et al 1991) where H_2S and Sn^{2-} reacts with either greigite or mackinawite. An aqueous cluster of FeS is a common reactant between these two reactions (4 and 5) (Ricard & Morse 2005) which is formed by the dissolution of metastable iron sulfide (Wang & Morse 1996; Morse &Ricard 2004; Ricard & Luther 2007). Likewise, dissolved H_2S or HS^{-1} reacts with solid elemental S to give rise to polysulphide (Sn^{2-}) (Butler et al 2004).

3.2 Oxidizing conditions

The metastable iron sulfide and pyrite are oxidized by O_2 and Fe^{3+} which usually gives elemental S as a product under neutral conditions (Breemen 1973; Moses et al.1987; Evangelou & Zhang 1995; Ward et al.2004). O_2 is the oxidizing agent in PAS soils due to the circumneutral pH nature while Fe^{+3} in AS soil due to acidic nature (pH<4.5) (Arkesteyn 1980; Nordstrom 1980; Breemen 1982). Fe^{+3} has low solubility and concentration under circumneutral pH condition and cannot be used as an oxidizing agent in PAS soils (Schippers & Jørgensen 2001; Schippers & Jørgensen 2002). Different aerobic and anaerobic organisms such as thiobacilli group are responsible for the production of sulfate during the oxidation of reduced S compounds. The overall chemical reaction by thiobacilli group is represented by the equation 6 and 7. (Starkey 1966; Breemen et al. 1973.)

$$4FeS + 9O_2 + 10H_2O \rightarrow 4Fe(OH)_3 + 4H_2SO_4 \quad (6)$$

$$4FeS_2 + 15O_2 + 14H_2O \rightarrow 4Fe(OH)_3 + 8H_2SO_4 \quad (7)$$

In the above reactions (6 and 7) oxygen is the primary oxidant for metastable iron sulfide as well as for pyrite. This is because oxygen has already oxidized metastable iron sulfide completely in PAS soil, and the condition for Fe^{+3} as an oxidant is not favorable. (van Breemen et al. 1973.) Apart from these oxidants, there can be others such as MnO_2 (Schippers 2001; Jorgensen 2002.), which is usually low in Finnish AS soil (Aström & Björklund 1997; Österholm et al. 2002). Likewise, organic Sulphur is not contributing to acidification due to its very less share in Finnish AS and PAS soil (Purokoski 1958.)

3.3 Oxidation in PAS soil

In reaction 1 (TABLE 2), the oxidation of metastable iron sulfide leads to the formation of elemental S and $Fe(OH)_3$ in PAS soils (Wikilander et al. 1950; Puurokoski 1958). This elmental S reacts with the FeS (metastable iron sulfide) to form pyrite (FeS_2) (reaction 2 in TABLE 2) (Berner 1970). This reaction is also presented in equation 5 under reducing conditions, which occurs in an aqueous state (Butler et al. 2004). The thiobacilli bacteria (Sulphur oxidizing bacteria) is unable to oxidize elemental S completely due to neutral pH condition and low activity (Nordstrom et al. 1982). However, it oxidizes some part of elemental S formed (from equation 1, TABLE 2) as shown in reaction 3 (TABLE 2) (Starkey et al. 1966 & Nordstrom et al 1982).

During higher water level the sulfate produced (from reaction 3 in TABLE 2) reduces to metastable iron sulfide or to pyrite (Boman et al. 2008, 44-45). As already discussed in subsection 3.2 about Fe^{+3} as a secondary oxidant for pyrite and metastable iron sulfide (Schippers & Jørgensen et al. 2001; Schippers & Jørgensen et al. 2002). This can be illustrated by equation 6 (TABLE 2). The Fe^{+2} is oxidized to Fe^{+3} (reaction 6 in TABLE 2) in the presence of neutral pH environment and the further hydrolysis of Fe^{+3} (reaction 7 in TABLE 2) results in the precipitation as ferric hydroxide ($Fe(OH)_3$), decreasing the concentration of aqueous Fe^{+3} (Breemen et al. 1973; Nordstrom et al. 1982; Evangelou & Zhang et al. 1995). Thus, oxygen is the primary oxidant of pyrite (reaction 8, TABLE 2) but the initial oxidizing mechanism is quite slow (reaction 5 in TABLE 2) (Hart 1962; Bloomfield 1973). In Table 2 , FeS represents either makinawite or greigite (metastable iron sulfide). In the table PS=Parent Sediment (PAS soil), AH =Acid Horizon (AS soil), TZ=Transition Zone, PL=Plough Layer. Equation 4 is the overall reaction for equation 1 and 3. The equation 8 is the overall reaction between equation 3,5,6 and 7. The equation 11 is the overall reaction between equation 9 and 10

TABLE 2. Chemical reactions that occurs in Finnish acid soils (adapted from Boman et al. 2008)

Mechanisms in soil			Location
$8FeS+6O_2+12H_2O \rightarrow 8Fe(OH)_3+8S^0$		(1)	PS
$8FeS+8S^0 \rightarrow 8FeS_2$		(2)	PS
$8S^0+12O_2+8H_2O \rightarrow 16H^++8SO_4^{2-}$		(3)	PS,AH, TZ
$8FeS+18O_2+20H_2O \rightarrow 8Fe(OH)_3+16H^++8SO_4^{2-}$	(Reaction 1 and 3)	(4)	PS,AH,TZ
$4FeS_2+2O_2+8H^+ \rightarrow 4Fe^{2+}+4H_2O+8S^0$		(5)	PS,AH,TZ
$4Fe^{2+}+O_2+4H^+ \rightarrow 4Fe^{3+}+2H_2O$		(6)	PS,AH,TZ
$4Fe^{3+}+12H_2O \rightarrow 4Fe(OH)_3+12H^+$		(7)	PS,AH,TZ
$4FeS_2+15O_2+14H_2O \rightarrow 4Fe(OH)_3+16H^++8SO_4^{2-}$	(Reaction 3, 5 - 7)	(8)	PS,AH,TZ
$FeS_2+2Fe^{3+} \rightarrow 3Fe^{2+}+2S^0$		(9)	AH, TZ
$2S^0+12Fe^{3+}+8H_2O \rightarrow 12Fe^{2+}+16H^++2SO_4^{2-}$		(10)	AH, TZ
$FeS_2+14Fe^{3+}+8H_2O \rightarrow 15Fe^{2+}+16H^++2SO_4^{2-}$	(Reaction 9 and 10)	(11)	AH, TZ
$12FeS_2+45O_2+30H_2O+4K^+ \rightarrow 4KFe_3(SO_4)_2(OH)_6+36H^++16SO_4^{2-}$		(12)	AH
$KFe_3(SO_4)_2(OH)_6 \rightarrow 3FeOOH+K^++3H^++2SO_4^{-2}$		(13)	AH
$CaCO_3+H_2SO_4+H_2O \rightarrow CaSO_4 \cdot 2H_20+CO_2$		(14)	AH, PL

3.4 Oxidation in AS soil

Iron is present in trivalent form in oxidized material, while in neutral pH atmosphere iron is bounded with metastable iron sulfide or pyrite in bivalent form. Therefore Fe^{+3} is formed by the oxidation of Fe^{+2} (reaction 6 in TABLE 2) which further acts as an oxidizing agent in acidic soil. (Nordstrom et al. 1972.) Similarly, the formation of Fe^{+3} is further enhanced by thiobacilli bacteria which are active in the acidic phase, resulting in the acceleration of pyrite oxidation (Singer & Stumm 1970; Evangelou & Zhang 1995). Fe^{+3} produced by bacterial involvement have similar or faster kinetics than pyrite oxidation by Fe^{+3}, as shown in reaction 9 of table 2 (Nordstrom et al.1982).

In the acidic boundary, when pH is below 4.5, Fe^{+3} is easily soluble and work as S oxidant, resulting in the pyrite oxidation as in reaction 11 in table 2 (Nordstrom et al. 1982). In contrast, over a pH value of 3.5, Fe^{+3} is hydrolyzed and precipitates as Fe-hydroxides (Beemen et al. 1982), which is usual in Finnish AS soils (Palko et al.1994; Yli-Halla 1997; Mokma et al. 2000; Österholm et al. 2002; Sohlenius & Öborn 2004. Jarosite [$KFe_3(SO_4)_2(OH)_6$] is common mineral in AS soils in Finland, formed by the partial hydrolysis of Fe^{3+} during pyrite oxidation as shown in reaction 12 in Table 2 (Breemen et al. 1973, 2002) and jarosite upon hydrolysis forms goethite (FeOOH) as in reaction 13 in Table 2 (Breemen et al. 1982). Jarosite and schwertmannite [$Fe_8O_8(OH)_6SO_4$] are common in low coastal land in Australia under acidic (pH <4) environment (Sullivan & Bush 2004; Burton et al 2006c; Burton et al. 2007). To utilize acidic land as cultivable, lime is used as a neutralizing agent, and consequently, gypsum ($CaSO_4 \cdot 2H_2O$) is obtained in the product as in reaction 14 in Table 2 (Dent 1986). Superficially, the land is cultivable, but underneath the acidic situation continues and causes environmental hazards (Boman et al. 2008, 46).

4 ENVIRONMENTAL RISKS AND METAL MOBILIZATION

In this section, the different kinds of elements with their possibility to occur in acid sulfate soil are presented. The mobilization of these elements from acid sulfate soil to water sources, plants, and human beings is discussed. Similarly, the adverse effect on the environment, including human beings from the mobilization of these elements is further discussed.

4.1 Elements in AS soil

Aluminum (Al) is the third most abundant element in the earth's crust (Gupta et al. 2013) and found in alumino-silicate and Al-hydroxide form in Finnish AS soils (Fältmarsch, Åström & Vuori 2008, 445-446). As the pH decreases below 5, silicon is leached while the unstable solid form of aluminum oxy-hydroxide is left behind. This unstable form releases Al^{+3} to the soil, which further leads to toxicity. (Abate, Hussien, Laing & Mengistu 2013, 711–722.) The acidification (pH 2.5-4.5) facilitates the alumino-silicate weathering, Al-hydroxide dissolution, and Al-solubilization and transportation (Fältmarsch et al. 2008). Al hydrolysis further enhances acidification, and thus metals are leached to the soil. (Palko et al. 1994.) For example, the environmental conditions such as rainfall, snow melting, and additional acidification by Al-hydroxide leads to the transportation of metals such as Co, Ni, Zn, Cd, and Mn (Sohlenius et al. 2004). Åström and Björklund 1996; Åström 2001a, 2001b; Roos and Åström 2005; Österholm et al. 2005, observed that the concentration of these metals increased up to 50, 30, 20, 10, and 30 times than usual. These metals are usually found in the cationic fraction in water (Åström and Corin 2000). The overall discharge of metals from Finnish AS soils is much larger than entire industry as shown in Figure 2.

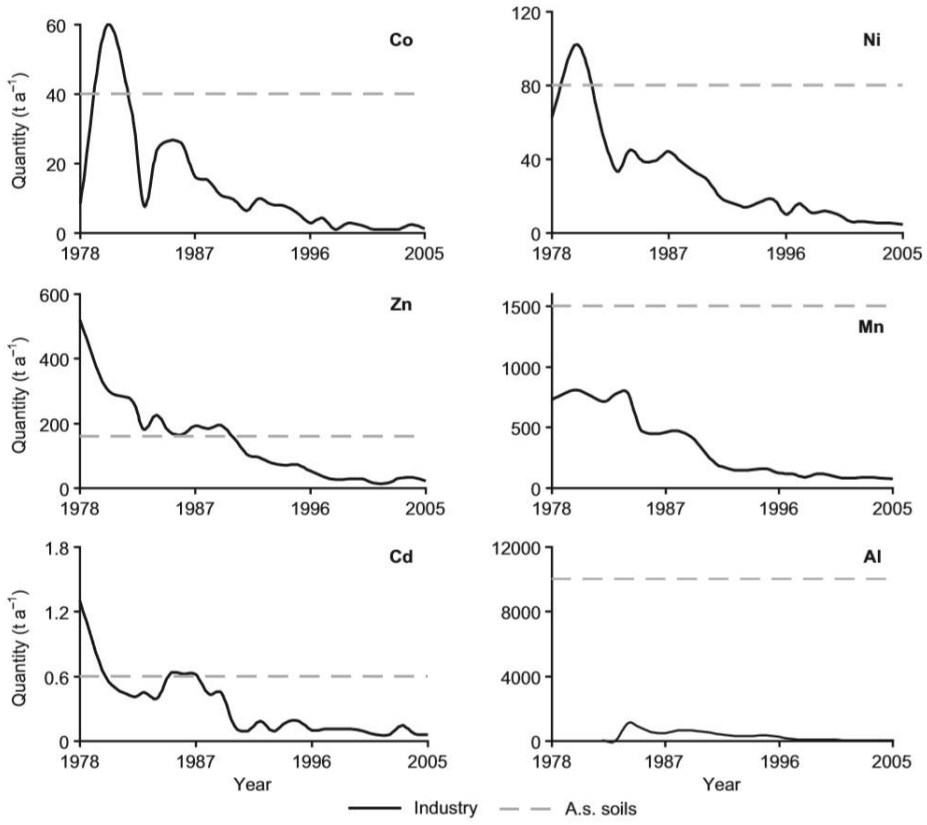

FIGURE 2. Figure representing leaching of metals from Finnish rivers and industries. (adapted from Sundström, Åström & österholm 2002)

Iron is usually found in sulfide form and precipitated as insoluble Fe-hydroxide (Åström et al. 2000). Even though iron is not leached out excessively from AS soils in comparison with glacial till and peat soils, increased concentration up to 100 mgl^{-1} have been found by Åström et al. 2000 in water draining through AS soils with pH 2.5-3.0 in anionic fraction. Likewise, chromium is also found in anionic form as iron (Lahermo et al. 1996; Åström et al 2000) and it is active in AS soils up to a certain level by the action of acidification and oxidation because it is less soluble in comparison with Zn, Co, Ni, Mn, and Cu (Palko & Yli-Halla 1990). The cultivable part of AS soils of Finland consists of higher concentration of Mg while that of P, K, Ca are in accordance with like Finnish average values (FAV) (Erviö & Palko 1984). The use of lime and mineral fertilizer for cultivation enables the probability of P and Ca higher (Österholm et al. 2002). The transportation of K, Mg, and Ca vary from small to large, while P is usually moderate (Åström 1998). A plentiful amount of Mg, Ca and K are found in water draining from AS soil which is shown by hydrogeochemical studies (Åström et al. 1995; Åström & Åström 1997). P and Mg are easily dissolved while K and Ca are poorly dissolved minerals. (Fältmarsch et al. 2008.)

4.2 Metals mobilization in crops

For the appropriate functioning of human body varieties of micronutrients elements such as nitrogen, phosphate, potassium, sulfur and the small proportion of micronutrients ions such as manganese, zinc, nickel, copper, iron, molybdenum, boron, chloride and copper are needed. The plant source is the main gateway to these nutrients for a healthy life. However, the consumption of these micro-nutrients in excess amount might lead to severe health issues such as abnormal growth and chlorosis. (Guterres, Rossato, Doley, & Pudmenzky 2018, 449.) The high content of metals can be observed in plants growing in acid sulfate soil and prevent the plant from its optimum growth (Yli-Halla, Virtanen, Mäkelä, Simojoki, Hirvi, Innanen, Mäkelä, & Sullivan 2017, 333-340).

A field study was done in various agricultural regions in the coastal area of Finland and elevated concentrations of Ni, Co, Al, Mn, and Cr were observed by Palko (1986,) in timothy plant. Likewise, and Yli-Halla and Palko (1987) found the concentrations of Fe, Mn, Co and Ni higher in oat grains in the same area as compared to Finnish Average Value (FAV). The plant roots absorb Fe by mobilizing its oxide bound form. Further, plants can absorb the dissolved form of heavy metals from roots. (Guterres et al. 2018, 462.) Likewise, Mn oxidizes the Cr^{+3} to Cr^{+6} which is mobile, easily soluble in water and highly toxic (Jaishankar et al. 2014, 60-62).

4.3 Impacts on aquatic habitats

The metal contamination in water sources results in the change in physicochemical properties of sediments, water and fish species (Baby, Raj, Biby, Sankarganesh, Jeevitha, Ajisha & Rajan 2010) and flora and fauna (Fatima & Usmani 2013). The metals leached to water sources bind to the surface of aquatic animals (Spicer and Weber, 1991) and are further transported to the cell interior (Christ et al. 1998). The blood plasma facilitates the movement of metals and is deposited on the liver, kidney, and various parts of an organism (Bentley 1991). The AS soil makes the water acidic with an adequate amount of metals, which causes an imbalance in aquatic habitats. The degradation of the quality of male and female reproductive cells (sperm and yolk) and the ability to lay eggs is disturbed by acidification. (Jezierska, Ługowska & Witeska 2009.) The gills of the aquatic animals such as fish, micro invertebrates and amphibians are directly affected by the contaminated water (U.S EPA 2011). For instance, the dissolved form of Al can block gills of aquatic habitats and decrease the ability to exchange gases (Nystrand, Österholm, Yu & Åström 2016).

The physiological and biological status of tissues and blood is further disturbed and causes cancer in fish (Pandey & Madhuri 2014, 17-23). It was found by Schuldermann et al. (2003) and Wang et al. (2013) that fish muscles contain the lowest amount of metals compared to liver, kidney and gills. The overall preference of metals for live fish was found to be Fe > Zn > Pb > Cu > Cd > Hg in laboratory and field experiment by Wang et al. (2013) and Yamazaki et al. (1996). However, this preference further depends upon fish species (Zhou et al. 1998), pH, salinity (Baldisserotto et al. 2004) as well as age and size of fish (Grieb et al. 1990). In an experiment conducted in India, it was noticed that the concentration of metals such as Cu, Cd, and Pb is higher in fish at high-temperature (Biswas et al. 2012) and low pH conditions (Çoğun & Kargın 2004).

4.4 Impacts on human beings

The acid sulfate soil is considered as the source for greenhouse gases and sulfur dioxide, which pollutes the environment and indirectly affect human health. The metals from acid sulfate soil can easily leach to groundwater which could further cause several diseases if used without proper treatment. Acidification facilitates acid-tolerant mosquito to carry ross river virus, which causes several diseases with joint pain and disabilities. (Ljung, Maley, Cook, & Weinstein 2009, 1238.) The excess of metals in the human body could lead to several neurological disorders (Zeitoun & Mehana 2014, 221) such as Alzheimer's disease resulted from a higher level of aluminum in the brain (Jaishankar et al. 2014, 65). Excess in the level of aluminum can lead to skin ulcers and mouth ulcers (Clayton 1989). Likewise, the exposure to metals such as Fe-Cu, Pb-Fe, Cu-Pb could lead to another neurological disease called Parkinson's Disease (Gorell et al. 1997, 1998, 1999; Gorell & Checkoway 2001).

In two-year (1991 and 1992), investigation of cow's milk by Alhonen (1997), cows were feeding on plants cultivated in AS soils affected area (basin of Kyrönjoki river), it was noticed that the concentration of zinc and iron were 2 folds in indoor feeding. While the concentration of aluminum was 50 folds in outdoor grazing of cows as compared to Finnish Average value (FAV). These metals find way to human beings through a pattern of plant - animals - human beings. The metals from AS soils to human beings is further presented in Figure 3. The increase in the concentration of iron in human cells forms free radical when iron is unable to bind to a protein. Iron enters to heart, liver and brain cells, produces acidity by releasing H^+ ion when Fe^{+2} is oxidized to Fe^{+3} and damages cellular organelles. (Albresten, 2006). Apart from these, soil contamination further affects cultural and traditional practices, emotional aspects as well as recreational activities such as boating and fishing (Ljung et al. 2009, 1239).

Similarly, the elevated level of cadmium (4 folds in unpolished rice grain) was noticed in rice grains in Japan, which were further consumed by human beings resulting in a severe disease called 'Itai-Itai.' The people suffering from this disease could not move, and thus, they could only say itai- itai, which means 'it hurts'- 'it hurts'. The reduction in the vegetation and aquatic habitats were noticed in the same area. (Aoshima 2016, 319-326.) Cadmium can further cause skeletal damage and is deposited in the kidney at low concentrations. It can also get into the body through smoking as tobacco plant accumulates cadmium. (Järup 2003, 167-182.) Similarly, exposure to lead (Pb) can lead to loss of appetite, headache, hypertension, abdominal pain, hallucinations, congenital disabilities, paralysis and even death (Jaishankar et al. 2014, 67-68).

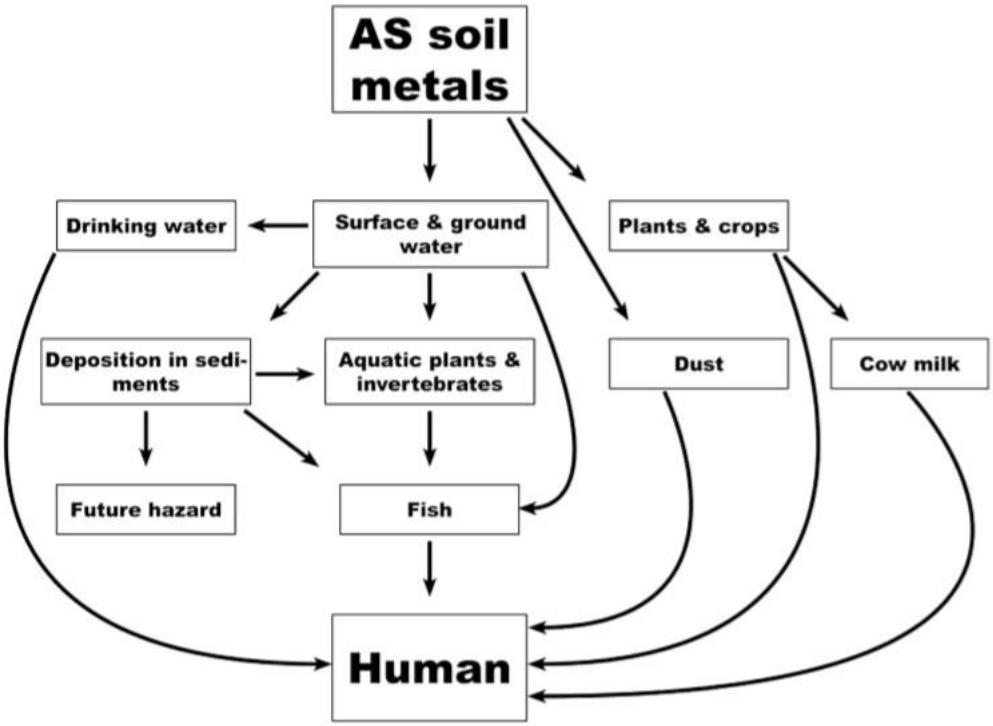

FIGURE 3. Probabilities of possible exposure of metals from acid sulphate soil to human beings through biological pathway (adapted from Fältmarsch 2010)

5 MANAGEMENT OF ACID SULFATE SOILS

The decrease in the groundwater level facilitates the formation of acid sulphate soils. For example, in Finland, groundwater level increases in spring when the snow melts, while in summer it decreases. From the application of Control Subsurface Drainage (CD) and Control Subsurface Irrigation (CDI) as shown in the Picture 7, the acidification of soil can be prevented. These technologies have been used in Finland since 1990. The system consists of a floating plastic antenna and foam base which floats vertically as the groundwater varies and thus provides information about the groundwater level. The system further consists of a flow measuring system (EHP ultrasonic flow monitoring system) in control well, which monitors the water flow in drainage outlets. The vertical plastic sheet is arranged between the field to avoid the leakage of water. During excess water condition in spring, water can be drained to the main drain and during low water condition in summer, water can be pumped from the main drain to raise the groundwater level artificially as in Picture 7. (Österholm, Virtanen, Rosendahl, Uusi-Kämppä, Ylivainio, Yli-Halla, Mäensivu & Turtola 2015, 110-113.)

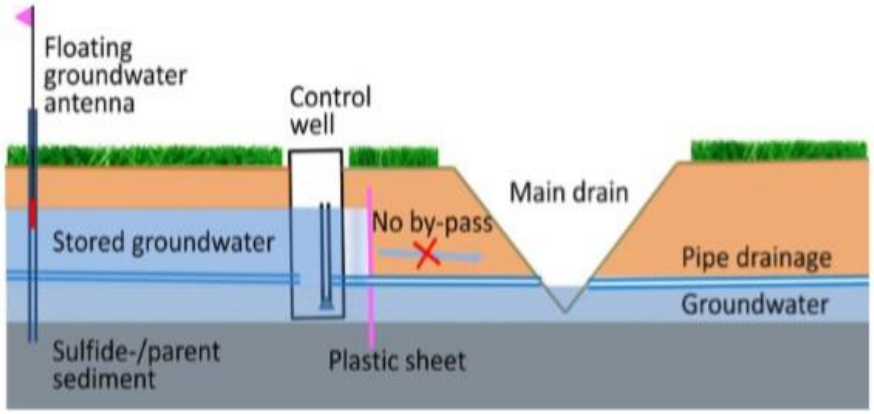

PICTURE 7. Control Sub-surface and Control Subsurface Irrigation technology. (adapted from Österholm et al. 2015)

6 SAMPLING

Soil samples were taken from Finnish AS and PAS soils as marked in Figure 13 with star sign to analyze the leached concentration of metals such as Co, Li, Ni and Zn from an acid sulfate soil to water in a small-scale lab experiment. The data set consists of 23 soil samples provided by GTK which were analyzed in AAS experiment at Centria UAS. These samples had already been analyzed for metals and trace elements by Labtium. There are altogether 14 soil profiles namely GK_KADA-2018-21, GK_KADA-2018-27, GK_ KADA-2018-26, GK_KADA-2018-23, GK_KADA-2918-25, GK_KADA-2018-22, GK_KADA-2018-24, GK_KADA-2018-20, GK_KADA-2018-28, GK_KADA-2018-31, GK_KADA-2018-30, GK_KADA-2018-29, GK_KADA-2018-30 and GK_KADA-2018-31.The soil profile of GK_KADA-2018-30 and GK_KADA-2018-31 consists of sub- samples which are presented in Table 4.From all these profiles the field depth, field pH and incubation pH was previously measured by GTK and shown in table 4 under the data and calculation section.

PICTURE 8. Several sampling points marked with star sign from Finnish acid sulfate soil.

7 METHODOLOGY AND EXPERIMENTAL PROCEDURE

Most of the initial setup for the experiment such as arranging and numbering samples, centrifugation and syringe filtration took place at Geological Survey of Finland while AAS experiment took place at Centria UAS. All the mathematical equations used for the calculation are presented under the sub-section methodology while the experimental procedure is presented under the subsection 7.2.

7.1 Methodology

This sub-section contains all the formulas used for the calculation of results. At first the dry weight was calculated by using the equation as shown in equation 8. PC represents the weight of porcelain cup while PC+S represents the combined weight of porcelain cup and soil sample after drying overnight in oven to get the dry weight amount. The dry weight concentration can be calculated using equation 9 where dry weight obtained from equation 8 is divided by combined weight of soil and water which is further multiplied by 100 %. Now the amount of water concentration present in a sample was obtained by subtracting dry weight concentration obtained from equation 9 from 100 % as shown in equation 10. The dry weight is the overall dry weight of the soil sample obtained by multiplying dry weight (obtained by drying a portion of sample overnight in oven from equation 8) with total sample amount or mass as shown in equation 11.

$$\text{Dry weight} = (PC+S)\ \text{g} - (PC)\ \text{g} \tag{8}$$

$$\text{Dry weight concentration} = \frac{\text{Dry weight}}{\text{weight of soil + water}} \cdot 100\% \tag{9}$$

$$\text{Water Concentration} = 100\% - \text{Dry weight concentration} \tag{10}$$

$$\text{Dry weight in sample} = \text{Dry weight} \cdot \text{Sample amount} \tag{11}$$

Similarly, the mass of metals present in dry sample obtained from equation 11 was calculated by multiplying the amount of metal (which is already known) with dry weight of sample divided by 1000 as shown in equation 12. For the calculation of metals leached from soil to water, 40 ml or 0.4L of de ionized water which was transferred to the incubation tube was multiplied with the mean value obtained from AAS lab results as shown in equation 13.Finally, metals from soil to water percentage was obtained by dividing the mass of metal in water by the mass of metal in sample as shown in equation 14.

$$\text{Metal mass} = \frac{\text{Amount of metal} \cdot \text{ Dry weight of sample}}{1000} \quad (12)$$

$$\text{Mass of metal leached} = 0{,}04\ \text{L} \cdot \text{ mean value from AAS} \quad (13)$$

$$\text{Metals from soil to water} = \frac{\text{mass of metal in water}}{\text{mass of metal in sample}} \quad (14)$$

7.2 Preparation of samples

The samples were collected from Finnish AS and PAS soil and oxidized for several months as shown in A (PICTURE 9). The samples were sprayed with water and mixed very well by a glass tube, and then the incubation pH was measured with a pH meter. The weight of the empty porcelain cup was measured, and then a portion of the sprayed sample was transferred in the oven to dry overnight. The remaining samples were then transferred to the incubation tube as shown in B (PICTURE 9), and the weight of the sample transferred was measured as in C (PICTURE 9). 40 ml of de-ionized water was then transferred to the incubation tube as in D (PICTURE 9) and was stirred overnight by a magnetic stirrer as in E (PICTURE 9). After stirring overnight, the incubation tubes were transferred to centrifuge (Eppendorf centrifuge 5804) as in F (PICTURE 9) at 3000 rpm for 3 minutes for sedimentation of the solid mixed

mass. Some samples were centrifuged for 4 minutes. Similarly, the dried porcelain cup samples were then transferred to the execator for a while. The weight of the dried samples was further measured.

New centrifuge tubes were numbered, and the solution (watery liquid) present in the centrifuge tube after centrifuge was sucked up by the syringe as in G (PICTURE 9) and transferred to new centrifuge tube after filtration (Hydrophilic PES 0,45 µm) as in H (PICTURE 9). This new centrifuge tube was rinsed twice with the solution before transferring the sucked solution. 5 ml of solution was taken as a reference to measure the pH while the remaining samples were acidified by adding two drops of nitric acid.

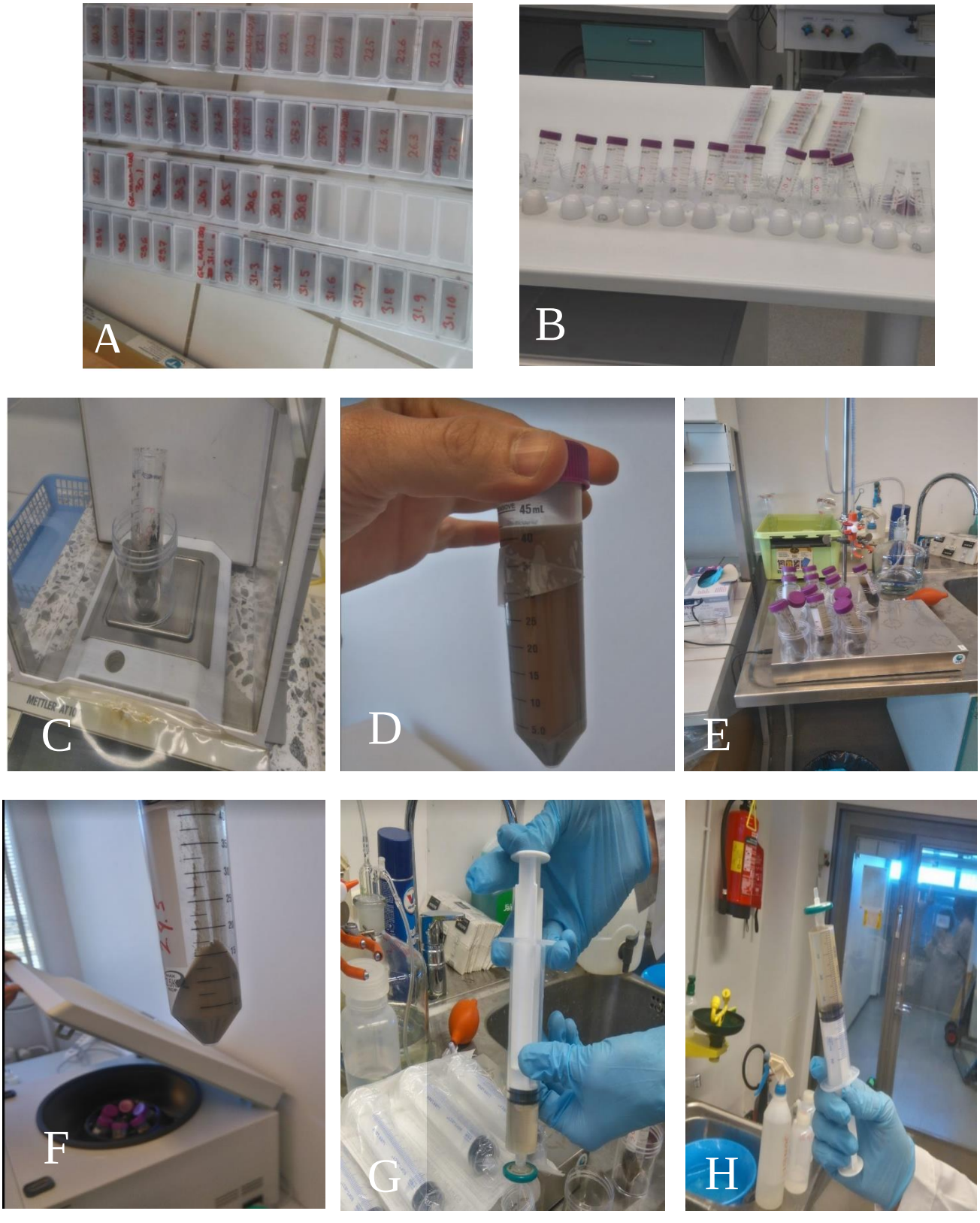

PICTURE 9. Representation of the lab experiment procedure in pictures.

7.3 AAS test

The standard solution for nickel, cobalt, lithium, and zinc was prepared in 1000 ml of round bottom flask. Similarly, the required amount of the solution for nickel, cobalt, lithium, and zinc was further transferred from 1000 ml standard solution to 100 ml round bottom flask. The data representing the solution transferred to a 100 ml bottle is presented in Table 3. The readings obtained from the AAS experiment are presented in the Results section.

TABLE 3. The range for metals cobalt (Co), nickel (Ni), lithium (Li) and zinc (Zn) with their range in ppm.

Metals	ppm	ppm	ppm
Co	0,03	0,2	2
Ni	0,02	3	10
Li	0,01	0,5	3
Zn	0,05	0,5	2

8 RESULTS AND DISCUSSION

This section consists of the results obtained from the lab experiment. The section consists of 23 soil profiles presented in table and their corresponding values of pH, metals available in soil samples, metals leached to water and metals percentage leached. Similarly, graph for pH, metals available in soil samples, metals leached to water and their percentage for soil profile GK_KADA_2018.30 and GK_KADA_2018.301 are further presented.

8.1 pH graph

The results obtained from the measurement of field pH and incubation pH are presented in Table 4 while the soil profiles GK_KADA-2018-30 and GK_KADA-2018-31 are presented in Figure 4 a and b respectively. In Table 4, 23 soil profiles are presented with their respective incubation pH and field pH. These soil samples were taken from the depth range of 0-2 meters. Incubation pH was measured at GTK lab after the preservation of these soil samples for several months while the field pH was measured at the field from where samples were taken. Blue and red color indications represent soil profile GK_KADA-2018-30 and GK_KADA-2018-31 which are further presented in Figure 4 (a and b).

TABLE 4. The representation of the 23 soil profiles with their respective depth, field pH and incubation pH.

Samples	Depth (m)	Incubation pH	Field pH
GK_KADA-2018-20.4	0,6-0,8	6,4	7
GK_KADA-2018-21.4	0,6-0,8	6	5,4
GK_KADA-2018-22.6	1,3-1,5	4,7	5,6
GK_KADA-2018-23.5	1-1,2	5,9	6,7
GK_KADA-2018-24.4	0,55-0,7	3,1	4,6
GK_KADA-2018-24.5	0,7-0,9	4,3	6
GK_KADA-2018-24.7	1,1-1,3	4,8	6,2
GK_KADA-2018-25.4	0,6-0,8	4,8	4,8
GK_KADA-2018-26.3	0,55-0,7	5,4	5,3
GK_KADA-2018-27.3	0,3-0,5	5,5	5,5

TABLE 4.(continues)

Samples	Depth (m)	Incubation pH	Field pH
GK_KADA-2018-28.3	0,6-0,8	6,1	5,5
GK_KADA-2018-29.7	1,2-1,4	5.9	5.3
GK_KADA-2018-30.1	0-0,2	4,6	3,9
GK_KADA-2018-30.3	0,4-0,75	2,6	3,7
GK_KADA-2018-30.4	0,75-1	3,4	6,1
GK_KADA-2018-30.6	1,2-1,5	4	6,4
GK_KADA-2018-30.8	1,75-2	3,9	6,9
GK_KADA-2018-31.1	0-0,15	4,3	3,9
GK_KADA-2018-31.3	0,35-0,55	3,9	3,6
GK_KADA-2018-31.5	0,7-0,9	3,4	4,3
GK_KADA-2018-31.7	1,1-1,3	3,7	4,8
GK_KADA-2018-31.9	1,5-1,75	5,3	6,5
GK_KADA-2018-31.10	1,75-2	4,5	6,8

From Figure 2 a, clear distinction can be made between oxidized and reduced soils. The first two points at field pH curve having pH less than 4 falls under oxidized soil category while the last three points having pH over 6 falls under reduced soil category. Between the oxidized and reduced zone transition zone can be observed. Furthermore, it is observed that the difference between the field pH and incubation pH is higher in reduced soils as compared to oxidized soil. Likewise, from Figure 2 (b), the first four points at field pH curve falls under oxidized soil while the last two points falls under reduced soil group. Between these two different groups transition zone is observed. Furthermore, the difference of pH value among field pH and incubation pH at oxidized zone is less than compared to the reduced zone.

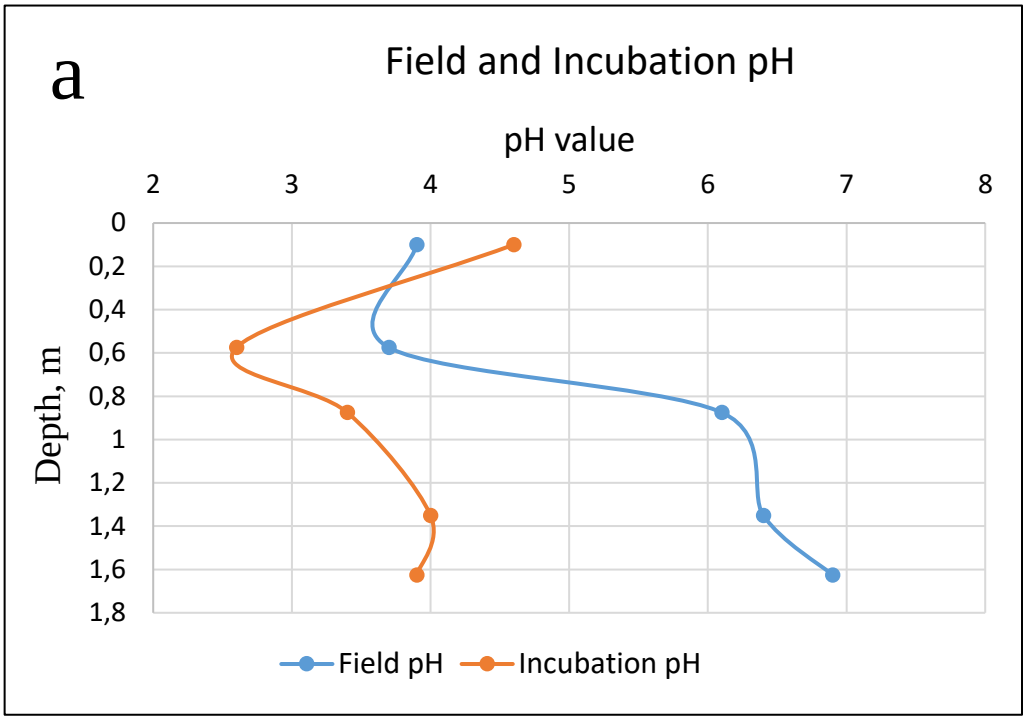

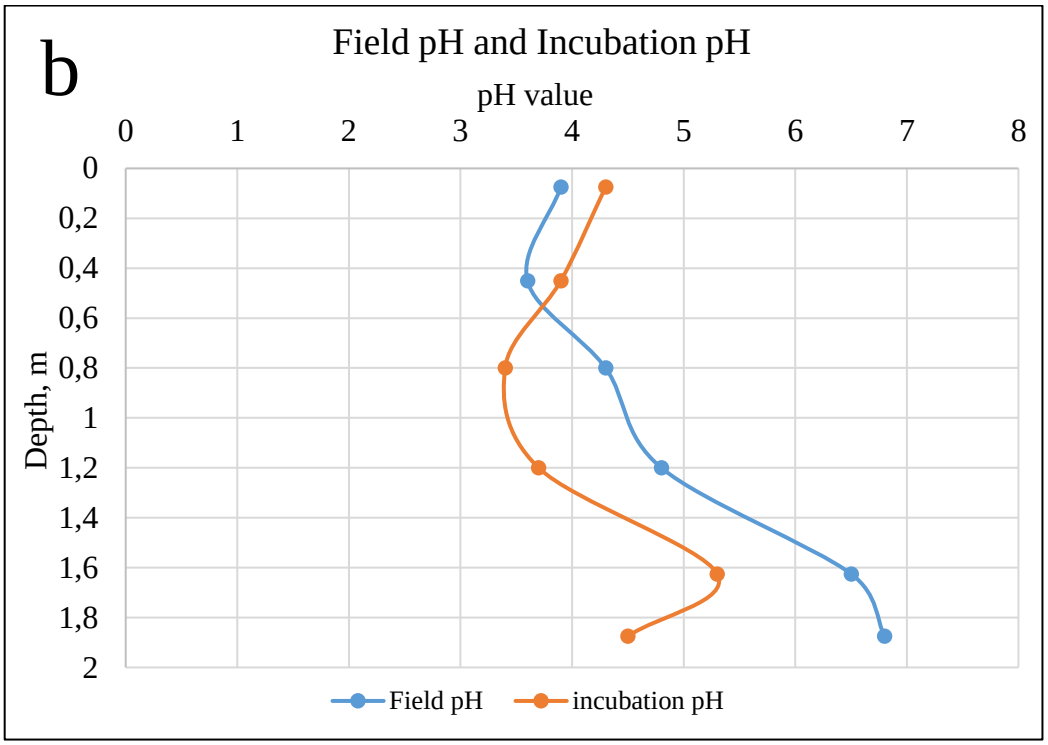

FIGURE 4. The graph represents the pH values of the field of incubation of soil profile a (GK_KADA_2018.30**)** and b (GK_KADA_2018.31.)

8.2 Metals available in soil sample

The given table represents the four different metal amounts present in a soil sample (Co, Li, Ni, and Zn). The lowest availability of metals for Co, Ni and Zn can be found in soil profile GK-KADA-2018-31.3 (TABLE 5) while for Li in profile GK-KADA-2018-31.5. On contrast, the highest availability of metals for Co, Li and Zn is found in soil profile GK-KADA-2018-24.5 (TABLE 5) while Ni in soil profile GK-KADA-2018-28.3. Blue and red color indications represent soil profile GK_KADA-2018-30 and GK_KADA-2018-31 and their metals availability is further presented in Figure 3(c and d). The grey color represents the highest value of metal in milligram while green color represents the lowest value. The red color symbol X represents the absence of value for further calculation.

TABLE 5. Representation of metals amount present in different soil profiles.

Samples	Co mg	Li mg	Ni mg	Zn mg
GK_KADA-2018-20.4	0,0514	0,1049	0,1199	0,3167
GK_KADA-2018-21.4	0,0130	0,0241	0,0815	0,0734
GK_KADA-2018-22.6	0,0617	0,0713	0,2385	0,2741
GK_KADA-2018-23.5	0,0605	0,1137	0,2110	0,3302
GK_KADA-2018-24.4	0,0153	0,0243	0,0701	0,0743
GK_KADA-2018-24.5	0,0956	0,2034	0,2148	0,6067
GK_KADA-2018-24.7	0,0707	0,1403	0,1715	0,4365
GK_KADA-2018-25.4	0,0323	0,0859	0,1967	0,2309
GK_KADA-2018-26.3	0,0093	0,0190	0,0663	0,0633
GK_KADA-2018-27.3	0,0198	0,0369	0,1665	0,1134
GK_KADA-2018-28.3	0,0268	0,0573	0,8089	0,1465
GK_KADA-2018-29.7	0,0135	0,0233	0,0436	0,0827
GK_KADA-2018-30.1	X	X	X	X
GK_KADA-2018-30.3	0,0212	0,0245	0,0718	0,0769
GK_KADA-2018-30.4	0,0186	0,0199	0,1253	0,0862
GK_KADA-2018-30.6	0,0293	0,0571	0,1184	0,1811
GK_KADA-2018-30.8	0,0639	0,1193	0,1579	0,4338
GK_KADA-2018-31.1	X	X	X	X

TABLE 5. (continues)

Samples	Co mg	Li mg	Ni mg	Zn mg
GK_KADA-2018-31.3	0,0054	0,0084	0,0343	0,0440
GK_KADA-2018-31.5	0,0072	0,0072	0,0455	0,0303
GK_KADA-2018-31.7	0,0209	0,0340	0,1001	0,1132
GK_KADA-2018-31.9	0,0255	0,0554	0,1192	0,1597
GK-KADA-2018.31.10	0,0594	0,1342	0,1483	0,4725

From the given Figure 5 c and d, metals amount for cobalt, lithium, nickel and zinc present in soil samples GK_KADA-2018-30 and GK_KADA-2018-31 can be known. The Figure 5 (c and d) refers to soil profile GK_KADA_2018.30 which consists of five sub-samples and GK_KADA_2018.31which consists of six sub-samples. The metals amount is found to be higher on reduced zone while lower at oxidized zone. zinc has the highest availability while cobalt is found to be in the least amount as shown in Figure 3 (c and d). The highest possibility of metals occurs at depth of 1,6- 1,8 meters for Figure (c) and 1,8-2 meters for Figure (d). In contrast the lowest availability of metals occurs at depth of 0- 0,2 meters (c and d).

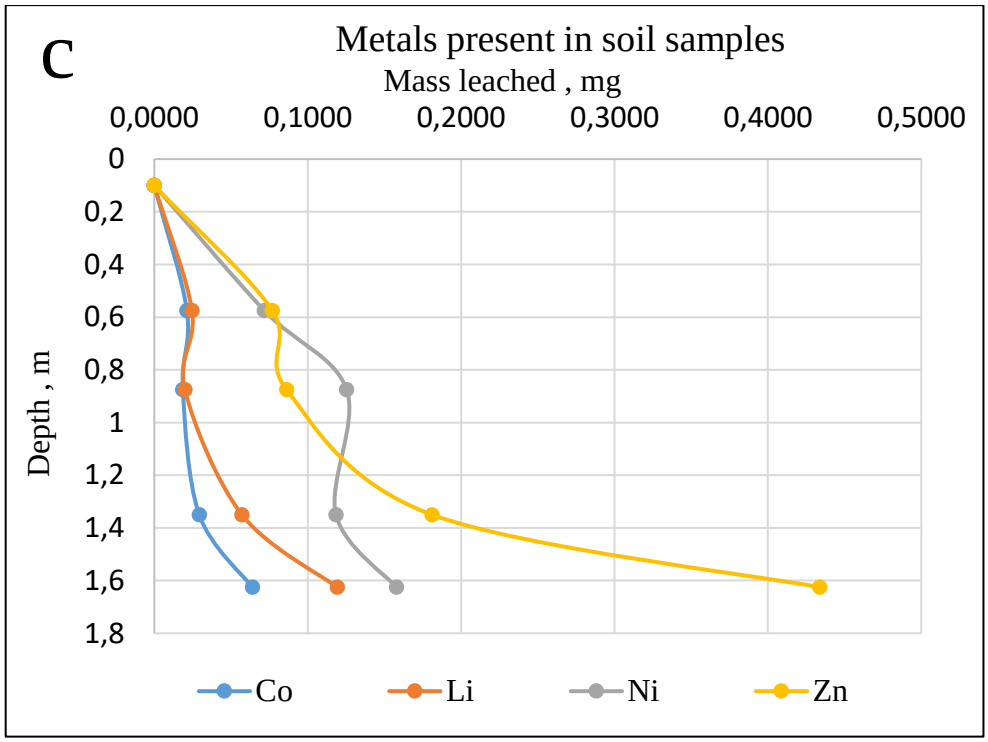

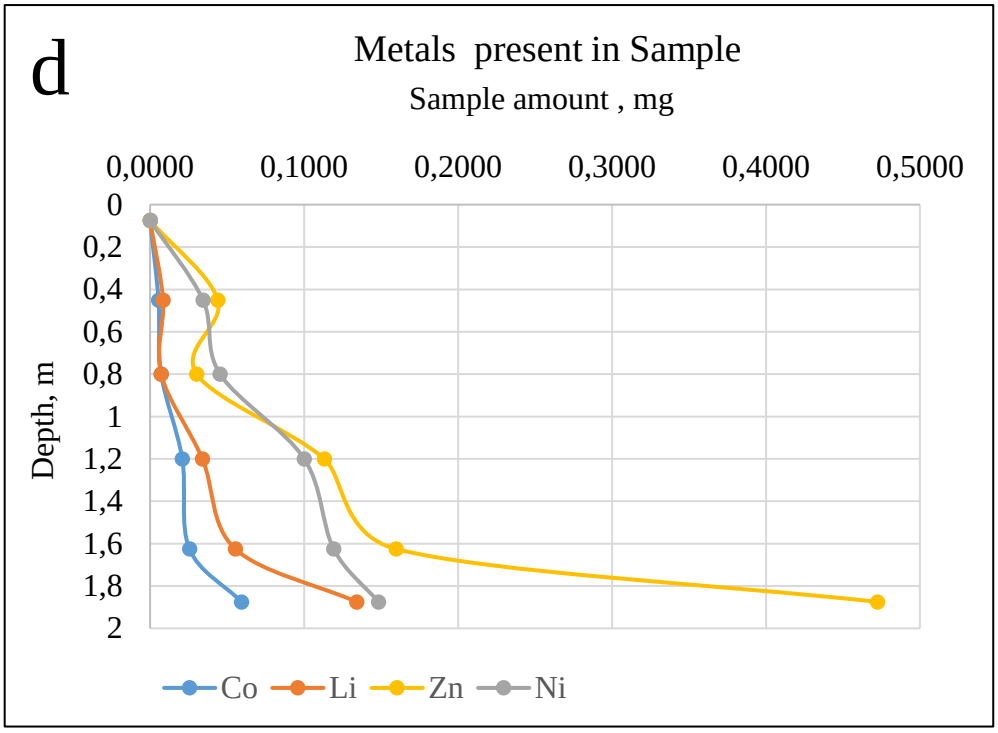

FIGURE 5. The graph represents the mass of metals (Co, Li, Ni and Zn) present in the soil profile GK_KADA_2018.30 and GK_KADA_2018.30**.**

8.3 Metals leached to water

The overall metals leached from soil to water from each soil profile is presented in Table 6. Blue and red color indications represent soil profile GK_KADA-2018-30 and GK_KADA-2018-31 which are further presented in Figure 6. The grey color represents the highest value of metal leached in milligram while green color represents the lowest value. The highest value of metals leached from soil to water for Co, Li, Ni and Zn are 0,0170, 0,0056, 0,0210 and 0,0284 respectively. In contrast the lowest value of metals leached to water for metals Co, Li, Ni and Zn are 0,0024, 0,0014, 0,0027 and 0 respectively.

TABLE 6. Representation of metals leached from soil to water in milligram.

Sample	Co leached mg	Li leached mg	Ni leached mg	Zn leached mg
GK_KADA-2018-20.4	0,0024	0,0019	0,0027	0
GK_KADA-2018-21.4	0,0025	0,0018	0,0043	0
GK_KADA-2018-22.6	0,0066	0,0020	0,0209	0,0048
GK_KADA-2018-23.5	0,0028	0,0014	0,0035	0
GK_KADA-2018-24.4	0,0064	0,0049	0,0170	0,0096
GK_KADA-2018-24.5	0,0064	0,0053	0,0140	0,0048
GK_KADA-2018-24.7	0,0042	0,0032	0,0077	0,0024
GK_KADA-2018-25.4	0,0028	0,0018	0,0112	0
GK_KADA-2018-26.3	0,0029	0,0016	0,0052	0
GK_KADA-2018-27.3	0,0029	0,0016	0,0047	0
GK_KADA-2018-28.3	0,0029	0,0017	0,0058	0
GK_KADA-2018-29.7	0,0028	0,0016	0,0030	0
GK_KADA-2018-30.1	0,0028	0,0015	0,0031	0
GK_KADA-2018-30.3	0,0170	0,0056	0,0504	0,0284
GK_KADA-2018-30.4	0,0063	0,0032	0,0208	0,0096
GK_KADA-2018-30.6	0,0063	0,0047	0,0123	0,0124
GK_KADA-2018-30.8	0,0088	0,0035	0,0210	0,0196
GK_KADA-2018-31.1	0,0032	0,0014	0,0032	0,0004
GK_KADA-2018-31.3	0,0034	0,0016	0,0056	0,0008
GK_KADA-2018-31.5	0,0048	0,0021	0,0112	0,0052

TABLE 6. (continues)

Sample	Co leached mg	Li leached mg	Ni leached mg	Zn leached mg
GK_KADA-2018-31.7	0,0067	0,0032	0,0130	0,0084
GK_KADA-2018-31.9	0,0062	0,0044	0,0112	0,0112
GK_KADA-2018-31.10	0,0024	0,0019	0,0027	0,0012

The given Figure 6 (e and f) represents the soil profile GK_KADA_2018.30 and GK_KADA_2018.30 which represents the metals amounts for Co, Li, Ni and Zn leached from soil to water. The metals are leached highly from oxidized zone than reduced zone among which nickel is effectively leached while lithium is ineffectively leached. From Figure 6 e metals are found to be extremely leached from depth of 0,4 -0,6 meters while ineffectively leached from depth of 1,6- 1,8 meters. Likewise, from figure 6 f zinc and lithium are hugely leached from depth of 1,6 -1,8 meters which is reduced zone while cobalt and zinc are highly leached from 1,2 meters which is oxidized zone. In contrast metals are feebly leached from 1,8-2,0 meters.

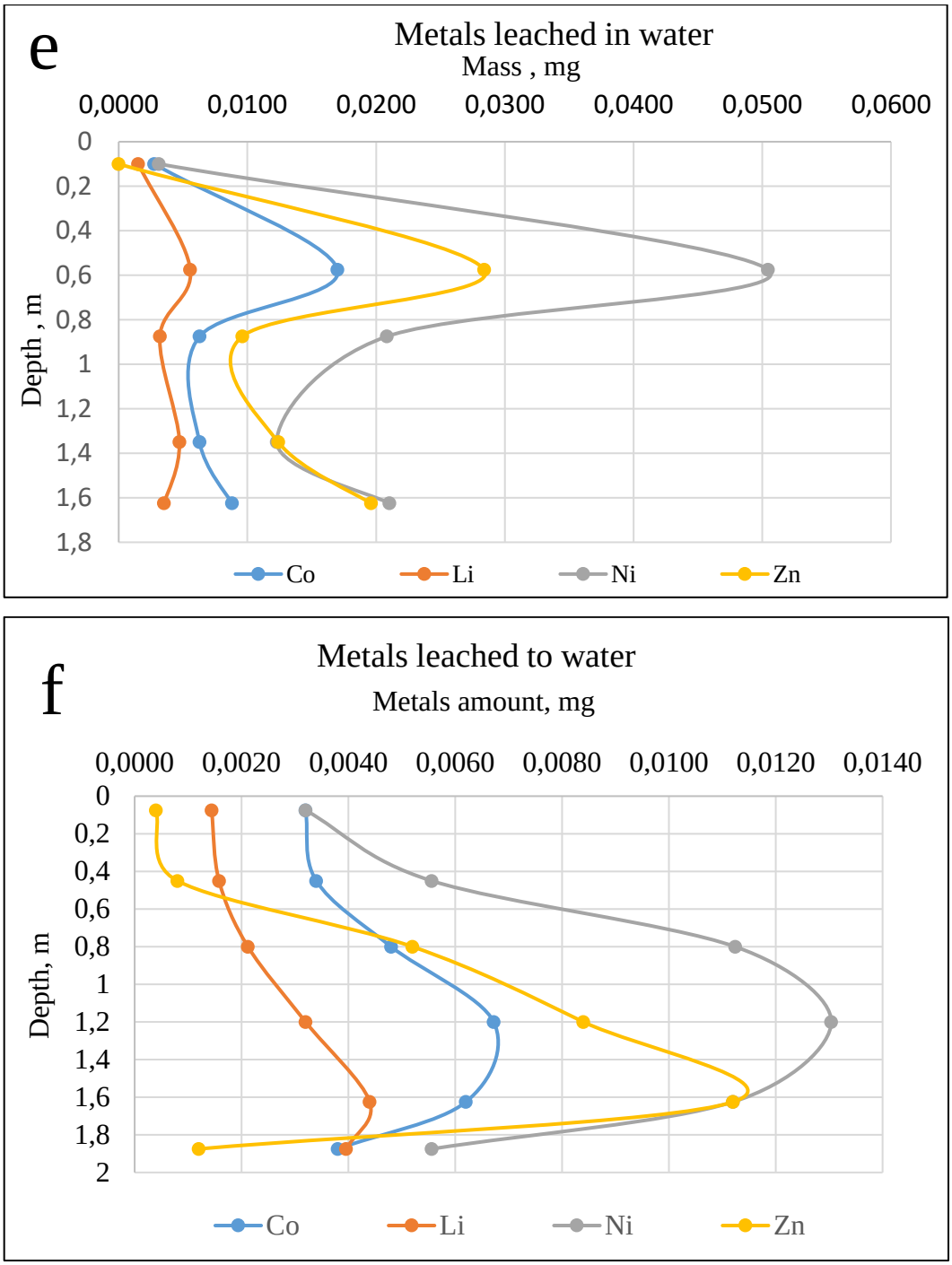

FIGURE 6. The graph represents the metals leached from soil samples (e and f) GK_KADA_2018.30 and GK_KADA_2018.31 to water.

8.4 Metals percentage

Metals leaching percentage from soil to water for all soil profiles is presented in Table 7. Blue and red color indications represent soil profile GK_KADA-2018-30 and GK_KADA-2018-31 which is further presented in Figure 5 (g and h). The grey color represents the highest value of metal leached in percentage while green color represents the lowest value. The red color symbol X represents the absence of value for further calculation. The highest percentage of metals leached for Co, Li, Ni and Zn are 80,0619, 29,5916, 70,2949 and 36,9406 respectively. In contrast the lowest percentage of leaching for Co, Li, Ni and Zn are 4,7470, 1,2309, 0,7219 and 0% respectively.

TABLE 7. Representation of metals leached percentage from soil to water.

Sample	Co leached %	Li leached %	Ni leached %	Zn leached %
GK_KADA-2018-20.4	4,7470	1,7926	2,2679	0,0000
GK_KADA-2018-21.4	19,3143	7,4573	5,2976	0,0000
GK_KADA-2018-22.6	10,7011	2,8624	8,7722	1,7511
GK_KADA-2018-23.5	4,6252	1,2309	1,6685	0,0000
GK_KADA-2018-24.4	41,6656	20,1310	24,2394	12,9277
GK_KADA-2018-24.5	6,7338	2,6253	6,4983	0,7912
GK_KADA-2018-24.7	5,8861	2,3092	4,4784	0,5498
GK_KADA-2018-25.4	8,7871	2,1425	5,7145	0,0000
GK_KADA-2018-26.3	30,8896	8,6407	7,9078	0,0000
GK_KADA-2018-27.3	14,7148	4,2330	2,8340	0,0000
GK_KADA-2018-28.3	10,9150	3,0004	0,7219	0,0000
GK_KADA-2018-29.7	20,3849	6,8617	6,7848	0,0000
GK_KADA-2018-30.1	X	X	X	X
GK_KADA-2018-30.3	80,0619	22,6676	70,2949	36,9406
GK_KADA-2018-30.4	33,8185	16,0836	16,6261	11,1348
GK_KADA-2018-30.6	21,4686	8,2646	10,3715	6,8477
GK_KADA-2018-30.8	13,7785	2,9506	13,3282	4,5180
GK_KADA-2018-31.1	X	X	X	X
GK_KADA-2018-31.3	62,4598	18,8665	16,1930	1,8196

TABLE 7.(continues)

Sample	Co leached %	Li leached %	Ni leached %	Zn leached %
GK_KADA-2018-31.5	66,9999	29,5916	24,7223	17,1560
GK_KADA-2018-31.7	32,1594	9,4240	13,0236	7,4214
GK_KADA-2018-31.9	24,2687	7,9491	9,3943	7,0144
GK_KADA-2018-31.10	6,3974	2,9505	3,7499	0,2540

The given Figure 7 g and h represents percentage leaching of metals Co, li, Ni and Zn for soil profiles GK_KADA_2018.30 and GK_KADA_2018.31respectively. It is noticed that metals from oxidized zones are leached more effectively while that of reduced zones are insufficiently leached. Cobalt is immensely leached while zinc is incompetently.

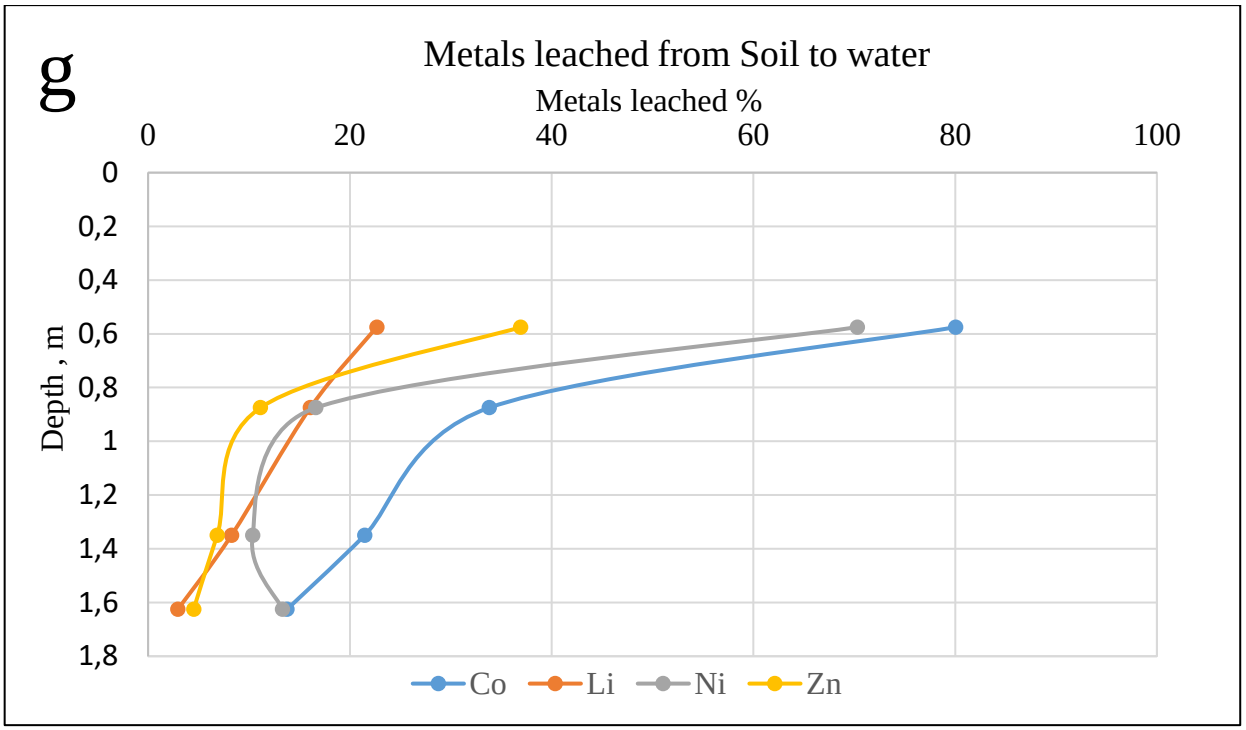

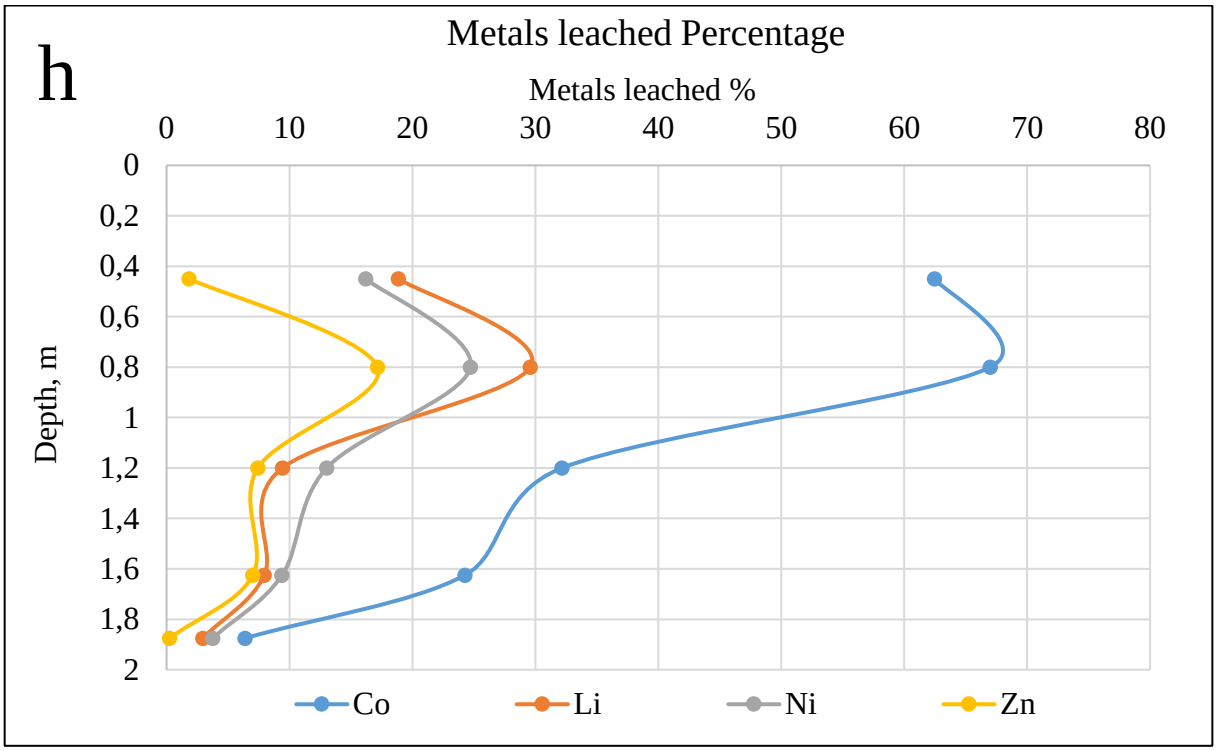

FIGURE 7. The percentage of metals Co, Li, Ni and Zn leached from soil samples GK_KADA_2018.30 and GK_KADA_2018.31 to water.

9 DATA AND CALCULATIONS

This section includes details of the overall calculation in five sub-sections which are basic data, metals available in soil sample, mass of metals in dry samples, metals leached from soil to water and their percentage. The calculated results from this section were used to obtain the Figure 2, 3,4 and 5 in results and discussion section.

9.1 Basic data

This sub-section includes required data for the further calculation of dry weight of sample, mass of metal in dry sample, metals leached from soil to water and their percentage. Blue and red color indications represent soil profile GK_KADA-2018-30 and GK_KADA-2018-31. For the abbreviations, PC represents the Porcelain Cup weight, S+W represents the collective weight of Sample (or soil) and Water, PC+S represents the weight of Porcelain Cup and Sample and S pH is Sample or Soil pH.

TABLE 8. The data for the calculation of mass of metals leached from AS soils to water.

Samples	PC g	S + W g	S g	PC +S g	S pH g
GK_KADA-2018-20.4	15,6274	1,1134	6,593	16,4149	6,4
GK_KADA-2018-21.4	14,5019	1,0931	3,7041	15,3825	6
GK_KADA-2018-22.6	15,6456	1,7607	9,5093	17,0869	4,7
GK_KADA-2018-23.5	16,4099	2,5911	8,4776	18,5738	5,9
GK_KADA-2018-24.4	16,536	0,9829	5,5871	17,2744	3,1

Samples	PC g	S + W g	S g	PC +S g	S pH g
GK_KADA-2018-24.5	15,9181	1,5436	6,9576	16,9439	4,3
GK_KADA-2018-24.7	15,7674	1,9098	7,6846	17,1199	4,8
GK_KADA-2018-25.4	16,0544	1,7166	7,149	17,3461	4,8
GK_KADA-2018-26.3	15,405	1,0844	3,9156	16,2554	5,4
GK_KADA-2018-27.3	15,449	1,8411	4,8081	16,923	5,5
GK_KADA-2018-28.3	16,4672	1,3057	5,9351	17,5404	6,1
GK_KADA-2018-29.7	15,9368	1,6957	5,515	17,3007	5,9
GK_KADA-2018-30.1	15,3806	0,3456	1,4551	15,6831	4,6
GK_KADA-2018-30.3	15,8421	1,1653	5,4813	16,51	2,6
GK_KADA-2018-30.4	16,0991	2,1792	3,8893	17,8043	3,4
GK_KADA-2018-30.6	15,4334	2,2692	8,0064	17,1732	4
GK_KADA-2018-30.8	16,2888	2,3105	6,8074	18,059	3,9
GK_KADA-2018-31.1	18,2405	0,4774	1,2993	18,5616	4,3

TABLE 8.(continues)

Samples	PC g	S + W g	S g	PC +S g	S pH g
GK_KADA-2018-31.3	16,498	1,114	3,7394	17,05789	3,9
GK_KADA-2018-31.5	15,2684	1,135	3,2254	16,1227	3,4
GK_KADA-2018-31.7	15,6236	1,7064	6,5033	16,9624	3,7
GK_KADA-2018-31.9	16,1875	2,0621	6,768	17,7603	5,3
GK_KADA-2018-31.10	16,7634	1,5904	4,0754	17,876	4,5

9.2 Dry weight of samples

In this sub section the calculation of metals available in soil samples is presented. In this step a portion of the sample was transferred to a known weight of porcelain cup (PC) and placed into oven to dry overnight. Then dry weight, dry weight concentration and water concentration were further calculated which leads to final dry weight present in sample.

9.2.1 Calculation of dry weight

The weight of porcelain cup was subtracted with the combined weight of porcelain cup and soil sample after drying overnight in oven to get the dry weight amount. The formula used for the calculation is stated in equation 8 in sub-section methodology 7.1. The highest dry weight obtained is 2,1639 grams while the lowest is 0,3025 grams. In Table 9, PC represents the porcelain cup weight and S represents the weight of sample. Blue and red color indications represent soil profile GK_KADA-2018-30 and GK_KADA-2018-31**.** The grey color represents the highest value while green color represents the lowest value**.**

TABLE 9. Calculation data of dry weight

Sample	PC +S weight g	PC weight g	Dry weight g
GK_KADA-2018-20.4	16,4149	15,6274	0,7875
GK_KADA-2018-21.4	15,3825	14,5019	0,8806
GK_KADA-2018-22.6	17,0869	15,6456	1,4413
GK_KADA-2018-23.5	18,5738	16,4099	2,1639
GK_KADA-2018-24.4	17,2744	16,536	0,7384
GK_KADA-2018-24.5	16,9439	15,9181	1,0258
GK_KADA-2018-24.7	17,1199	15,7674	1,3525
GK_KADA-2018-25.4	17,3461	16,0544	1,2917
GK_KADA-2018-26.3	16,2554	15,405	0,8504
GK_KADA-2018-27.3	16,923	15,449	1,4740
GK_KADA-2018-28.3	17,5404	16,4672	1,0732
GK_KADA-2018-29.7	17,3007	15,9368	1,3639

TABLE 9. (continues)

Sample	PC +S weight g	PC weight g	Dry weight g
GK_KADA-2018-30.1	15,6831	15,3806	0,3025
GK_KADA-2018-30.3	16,51	15,8421	0,6679
GK_KADA-2018-30.4	17,8043	16,0991	1,7052
GK_KADA-2018-30.6	17,1732	15,4334	1,7398
GK_KADA-2018-30.8	18,059	16,2888	1,7702
GK_KADA-2018-31.1	18,5616	18,2405	0,3211
GK_KADA-2018-31.3	17,05789	16,498	0,5599
GK_KADA-2018-31.5	16,1227	15,2684	0,8543
GK_KADA-2018-31.7	16,9624	15,6236	1,3388
GK_KADA-2018-31.9	17,7603	16,1875	1,5728
GK_KADA-2018-31.10	17,876	16,7634	1,1126

9.2.2 Dry weight concentration

After transferring a portion of sample to porcelain cup as described in sub heading 7,2 rest of the sample was transferred to known weight of incubation tube and the combined weight of soil and water (S+W) was obtained. The dry weight obtained by equation 8 was divided by the weight of soil and water multiplied by 100 to get the concentration of dry weight as shown by equation 9 in sub-section methodology 7.1. The highest dry weight concentration obtained was 87,5289 % while the lowest was 50,2594%. The blue and red color indications represent soil profile GK_KADA-2018-30 and GK_KADA-2018-31 while the grey color represents sample with the highest dry weight concentration while the green color represents the lowest concentration.

TABLE 10. The calculation of dry weight concentration.

Sample	S + W weight g	Dry Weight g	Dry weight concentration %
GK_KADA-2018-20.4	1,1134	0,7875	70,7293
GK_KADA-2018-21.4	1,0931	0,8806	80,5599
GK_KADA-2018-22.6	1,7607	1,4413	81,8595

TABLE 10. (continues)

Sample	S + W weight g	Dry Weight g	Dry weight concentration %
GK_KADA-2018-23.5	2,5911	2,1639	83,5128
GK_KADA-2018-24.4	0,9829	0,7384	75,1246
GK_KADA-2018-24.5	1,5436	1,0258	66,4550
GK_KADA-2018-24.7	1,9098	1,3525	70,8189
GK_KADA-2018-25.4	1,7166	1,2917	75,2476
GK_KADA-2018-26.3	1,0844	0,8504	78,4212
GK_KADA-2018-27.3	1,8411	1,474	80,0608
GK_KADA-2018-28.3	1,3057	1,0732	82,1935
GK_KADA-2018-29.7	1,6957	1,3639	80,4329
GK_KADA-2018-30.1	0,3456	0,3025	87,5289
GK_KADA-2018-30.3	1,1653	0,6679	57,3157
GK_KADA-2018-30.4	2,1792	1,7052	78,2489
GK_KADA-2018-30.6	2,2692	1,7398	76,6702
GK_KADA-2018-30.8	2,3105	1,7702	76,6155
GK_KADA-2018-31.1	0,4774	0,3211	67,2602
GK_KADA-2018-31.3	1,114	0,55989	50,2594
GK_KADA-2018-31.5	1,135	0,8543	75,2687
GK_KADA-2018-31.7	1,7064	1,3388	78,4576
GK_KADA-2018-31.9	2,0621	1,5728	76,2718
GK_KADA-2018-31.10	1,5904	1,1126	69,9572

9.2.3 Water concentration

After calculating the dry weight concentration from Table 10, the water concentration was obtained from equation 10 from sub-section methodology 7.1. The samples were preserved in laboratory for several months and therefore the water concentration in most of the samples was around 30 %. However, some samples water concentration was above 30 %, it was because the samples are not dried properly. The highest water concentration in a sample was found to be 49,7406 % while the lowest is 12,4711 %. In the given Table 11, blue and red color indications represent soil profile GK_KADA-2018-30 and

GK_KADA-2018-31 while grey color represents the highest water concentration and green for the lowest water concentration value.

TABLE 11. The water concentration obtained from dry weight.

Sample	Total %	Dry weight concentration %	water concentration %
GK_KADA-2018-20.4	100	70,7293	29,2707
GK_KADA-2018-21.4	100	80,5599	19,4401
GK_KADA-2018-22.6	100	81,8595	18,1405
GK_KADA-2018-23.5	100	83,5128	16,4872
GK_KADA-2018-24.4	100	75,1246	24,8754
GK_KADA-2018-24.5	100	66,4550	33,5450
GK_KADA-2018-24.7	100	70,8189	29,1811
GK_KADA-2018-25.4	100	75,2476	24,7524
GK_KADA-2018-26.3	100	78,4212	21,5788
GK_KADA-2018-27.3	100	80,0608	19,9392
GK_KADA-2018-28.3	100	82,1935	17,8065
GK_KADA-2018-29.7	100	80,4329	19,5671
GK_KADA-2018-30.1	100	87,5289	12,4711
GK_KADA-2018-30.3	100	57,3157	42,6843
GK_KADA-2018-30.4	100	78,2489	21,7511
GK_KADA-2018-30.6	100	76,6702	23,3298
GK_KADA-2018-30.8	100	76,6155	23,3845
GK_KADA-2018-31.1	100	67,2602	32,7398
GK_KADA-2018-31.3	100	50,2594	49,7406
GK_KADA-2018-31.5	100	75,2687	24,7313
GK_KADA-2018-31.7	100	78,4576	21,5424
GK_KADA-2018-31.9	100	76,2718	23,7282
GK_KADA-2018-31.10	100	69,9572	30,0428

9.2.4 Dry weight of sample

The dry weight of sample refers to the overall dry weight of the soil sample present in the incubating tube while the term dry weight refers to the portion of soil sample taken from incubation tube for drying overnight. Knowing the dry weight, the weight of total soil sample (S amount), dry weight in sample was calculated by the equation 11 from sub-section methodology 7.1. The highest dry weight of sample is found to be 18,3447 grams while the lowest is 0,4172 grams. In Table 13, S represents the total Sample or Soil. Blue and red color indications represent soil profile GK_KADA-2018-30 and GK_KADA-2018-31. The grey color represents the sample with highest dry weight while the green represents the lowest dry weight in grams.

TABLE 12. The table calculation data of dry weight of sample.

Sample	Dry weight g	S amount g	Dry weght of sample g
GK_KADA-2018-20.4	0,7875	6,593	5,1920
GK_KADA-2018-21.4	0,8806	3,7041	3,2618
GK_KADA-2018-22.6	1,4413	9,5093	13,7058
GK_KADA-2018-23.5	2,1639	8,4776	18,3447
GK_KADA-2018-24.4	0,7384	5,5871	4,1255
GK_KADA-2018-24.5	1,0258	6,9576	7,1371
GK_KADA-2018-24.7	1,3525	7,6846	10,3934
GK_KADA-2018-25.4	1,2917	7,149	9,2344
GK_KADA-2018-26.3	0,8504	3,9156	3,3298
GK_KADA-2018-27.3	1,474	4,8081	7,0871
GK_KADA-2018-28.3	1,0732	5,9351	6,3695
GK_KADA-2018-29.7	1,3639	5,515	7,5219
GK_KADA-2018-30.1	0,3025	1,4551	0,4402
GK_KADA-2018-30.3	0,6679	5,4813	3,6610
GK_KADA-2018-30.4	1,7052	3,8893	6,6320
GK_KADA-2018-30.6	1,7398	8,0064	13,9295
GK_KADA-2018-30.8	1,7702	6,8074	12,0505

TABLE 12. (continues)

Sample	Dry weight g	S amount g	Dry weght of sample g
GK_KADA-2018-31.1	0,3211	1,2993	0,4172
GK_KADA-2018-31.3	0,55989	3,7394	2,0937
GK_KADA-2018-31.5	0,8543	3,2254	2,7555
GK_KADA-2018-31.7	1,3388	6,5033	8,7066
GK_KADA-2018-31.9	1,5728	6,768	10,6447
GK_KADA-2018-31.10	1,1126	4,0754	4,5343

9.3 Mass of metal in dry sample

In this third step, mass of Co, Li, Ni and Zn metals present in dry weight of sample (from Table 12) were calculated using equation 12 from sub-section methodology 7.1. Here the milligram of cobalt, lithium, nickel and zinc per kilogram of soil (mg/kg) were already known which facilitate, the calculation of metal amounts.

9.3.1 Mass of cobalt

The highest mass of cobalt present in a dry sample was found to be 0,0956 milligram while the lowest was 0,0072 milligrams. Blue and red color indications represent soil profile GK_KADA-2018-30 and GK_KADA-2018-31. The grey color represents the highest value of Cobalt in milligram while green color represents the lowest value. The red color symbol X represents the absence of any value for further calculation. DW represents Dry Weight in gram while Co represents Cobalt.

TABLE 13. Mass of cobalt in dry sample.

Sample	DW of Sample g	Co (mg/kg)	Co mg
GK_KADA-2018-20.4	5,1920	9,9	0,0514
GK_KADA-2018-21.4	3,2618	4	0,0130
GK_KADA-2018-22.6	13,7058	4,5	0,0617
GK_KADA-2018-23.5	18,3447	3,3	0,0605

TABLE 13. (continues)

Sample	DW of Sample g	Co (mg/kg)	Co mg
GK_KADA-2018-24.4	4,1255	3,7	0,0153
GK_KADA-2018-24.5	7,1371	13,4	0,0956
GK_KADA-2018-24.7	10,3934	6,8	0,0707
GK_KADA-2018-25.4	9,2344	3,5	0,0323
GK_KADA-2018-26.3	3,3298	2,8	0,0093
GK_KADA-2018-27.3	7,0871	2,8	0,0198
GK_KADA-2018-28.3	6,3695	4,2	0,0268
GK_KADA-2018-29.7	7,5219	1,8	0,0135
GK_KADA-2018-30.1	0,4402	X	X
GK_KADA-2018-30.3	3,6610	5,8	0,0212
GK_KADA-2018-30.4	6,6320	2,8	0,0186
GK_KADA-2018-30.6	13,9295	2,1	0,0293
GK_KADA-2018-30.8	12,0505	5,3	0,0639
GK_KADA-2018-31.1	0,4172	X	X
GK_KADA-2018-31.3	2,0937	2,6	0,0054
GK_KADA-2018-31.5	2,7555	2,6	0,0072
GK_KADA-2018-31.7	8,7066	2,4	0,0209
GK_KADA-2018-31.9	10,6447	2,4	0,0255
GK_KADA-2018-31.10	4,5343	13,1	0,0594

9.3.2 Mass of lithium

The highest amount of lithium present in a dry sample was found to be 0,2034 milligrams while the lowest amount was 0,0072 milligrams. Blue and red color indications represent soil profile GK_KADA-2018-30 and GK_KADA-2018-31. The grey color represents the highest value of lithium in milligram while green color represents the lowest value. The red color symbol X represents the absence of value for further calculation. DW represents for Dry Weight in gram while Li represents Lithium.

TABLE 14. Mass of lithium in dry sample.

Sample	DW in Sample g	Li (mg/kg)	Li mg
GK_KADA-2018-20.4	5,1920	20,2	0,1049
GK_KADA-2018-21.4	3,2618	7,4	0,0241
GK_KADA-2018-22.6	13,7058	5,2	0,0713
GK_KADA-2018-23.5	18,3447	6,2	0,1137
GK_KADA-2018-24.4	4,1255	5,9	0,0243
GK_KADA-2018-24.5	7,1371	28,5	0,2034
GK_KADA-2018-24.7	10,3934	13,5	0,1403
GK_KADA-2018-25.4	9,2344	9,3	0,0859
GK_KADA-2018-26.3	3,3298	5,7	0,0190
GK_KADA-2018-27.3	7,0871	5,2	0,0369
GK_KADA-2018-28.3	6,3695	9	0,0573
GK_KADA-2018-29.7	7,5219	3,1	0,0233
GK_KADA-2018-30.1	0,4402	X	X
GK_KADA-2018-30.3	3,6610	6,7	0,0245
GK_KADA-2018-30.4	6,6320	3	0,0199
GK_KADA-2018-30.6	13,9295	4,1	0,0571
GK_KADA-2018-30.8	12,0505	9,9	0,1193
GK_KADA-2018-31.1	0,4172	X	X
GK_KADA-2018-31.3	2,0937	4	0,0084
GK_KADA-2018-31.5	2,7555	2,6	0,0072
GK_KADA-2018-31.7	8,7066	3,9	0,0340
GK_KADA-2018-31.9	10,6447	5,2	0,0554
GK_KADA-2018-31.10	4,5343	29,6	0,1342

9.3.3 Mass of nickel

The highest mass of nickel in a dry sample was found to be 0,8089 milligrams while the lowest is 0,0343 milligrams. Blue and red color indications represent soil profile GK_KADA-2018-30 and GK_KADA-2018-31. The grey color represents the highest value of nickel in milligrams while green color represents the lowest value. The red color symbol X represents the absence of value for further calculation. DW represents Dry Weight in gram while Ni represents nickel.

TABLE 15. Amount of nickel calculated in dry sample.

Sample	DW in sample g	Ni (mg/kg)	Ni mg
GK_KADA-2018-20.4	5,1920	23,1	0,1199
GK_KADA-2018-21.4	3,2618	25	0,0815
GK_KADA-2018-22.6	13,7058	17,4	0,2385
GK_KADA-2018-23.5	18,3447	11,5	0,2110
GK_KADA-2018-24.4	4,1255	17	0,0701
GK_KADA-2018-24.5	7,1371	30,1	0,2148
GK_KADA-2018-24.7	10,3934	16,5	0,1715
GK_KADA-2018-25.4	9,2344	21,3	0,1967
GK_KADA-2018-26.3	3,3298	19,9	0,0663
GK_KADA-2018-27.3	7,0871	23,5	0,1665
GK_KADA-2018-28.3	6,3695	127	0,8089
GK_KADA-2018-29.7	7,5219	5,8	0,0436
GK_KADA-2018-30.1	0,4402	X	X
GK_KADA-2018-30.3	3,6610	19,6	0,0718
GK_KADA-2018-30.4	6,6320	18,9	0,1253
GK_KADA-2018-30.6	13,9295	8,5	0,1184
GK_KADA-2018-30.8	12,0505	13,1	0,1579
GK_KADA-2018-31.1	0,4172	X	X
GK_KADA-2018-31.3	2,0937	16,4	0,0343
GK_KADA-2018-31.5	2,7555	16,5	0,0455
GK_KADA-2018-31.7	8,7066	11,5	0,1001

TABLE 15.(continues)

Sample	DW in sample g	Ni (mg/kg)	Ni mg
GK_KADA-2018-31.9	10,6447	11,2	0,1192
GK_KADA-2018-31.10	4,5343	32,7	0,1483

9.3.4 Mass of zinc

The highest mass of zinc present in a dry sample was found to be 0,6067 milligrams while the lowest was 0,0303 milligrams respectively. Blue and red color indications represent soil profile GK_KADA-2018-30 and GK_KADA-2018-31. The grey color represents the highest value of zinc in milligram while green color represents the lowest value. The red color symbol X represents the absence of value for further calculation. DW represents for Dry Weight in gram while Zn represents Zinc.

TABLE 16. Amount of zinc in dry sample.

Sample	DW in Sample g	Zn (mg/kg)	Zn mg
GK_KADA-2018-20.4	5,1920	61	0,3167
GK_KADA-2018-21.4	3,2618	22,5	0,0734
GK_KADA-2018-22.6	13,7058	20	0,2741
GK_KADA-2018-23.5	18,3447	18	0,3302
GK_KADA-2018-24.4	4,1255	18	0,0743
GK_KADA-2018-24.5	7,1371	85	0,6067
GK_KADA-2018-24.7	10,3934	42	0,4365
GK_KADA-2018-25.4	9,2344	25	0,2309
GK_KADA-2018-26.3	3,3298	19	0,0633
GK_KADA-2018-27.3	7,0871	16	0,1134
GK_KADA-2018-28.3	6,3695	23	0,1465
GK_KADA-2018-29.7	7,5219	11	0,0827
GK_KADA-2018-30.1	0,4402	X	X
GK_KADA-2018-30.3	3,6610	21	0,0769
GK_KADA-2018-30.4	6,6320	13	0,0862
GK_KADA-2018-30.6	13,9295	13	0,1811

TABLE 16.(continues)

Sample	DW in Sample g	Zn (mg/kg)	Zn mg
GK_KADA-2018-30.8	12,0505	36	0,4338
GK_KADA-2018-31.1	0,4172	X	X
GK_KADA-2018-31.3	2,0937	21	0,0440
GK_KADA-2018-31.5	2,7555	11	0,0303
GK_KADA-2018-31.7	8,7066	13	0,1132
GK_KADA-2018-31.9	10,6447	15	0,1597
GK_KADA-2018-31.10	4,5343	91	0,4725

9.4 Metals leached from soil to water

After the calculation of dry weight of sample, 40 ml of de ionized water was transferred to the incubation tube for facilitating the leaching of metals from soil to water. These samples with water were magnetically stirred, centrifuged, filtered and the clear water was transferred to another incubation tubes. Upon the AAS experiment of this samples, the leached mass was calculated.

9.4.1 Mean value from AAS

From the AAS experiment at Centria UAS laboratory, the following values of metals in samples were obtained. The lowest value of metal present is zero, which mostly occurred in zinc samples. Blue and red color indications represent soil profile GK_KADA-2018-30 and GK_KADA-2018-31.

TABLE 17. The metals value in ppm obtained from AAS analysis.

Sample	Co ppm	Li ppm	Ni ppm	Zn ppm
GK_KADA-2018-20.4	0,0610	0,0470	0,0680	0,0000
GK_KADA-2018-21.4	0,0630	0,0450	0,1080	0,0000
GK_KADA-2018-22.6	0,1650	0,0510	0,5230	0,1200
GK_KADA-2018-23.5	0,0700	0,0350	0,0880	0,0000
GK_KADA-2018-24.4	0,1590	0,1225	0,4250	0,2400

TABLE 17.(continues)

Sample	Co ppm	Li ppm	Ni ppm	Zn ppm
GK_KADA-2018-24.5	0,1610	0,1335	0,3490	0,1200
GK_KADA-2018-24.7	0,1040	0,0810	0,1920	0,0600
GK_KADA-2018-25.4	0,0710	0,0460	0,2810	0,0000
GK_KADA-2018-26.3	0,0720	0,0410	0,1310	0,0000
GK_KADA-2018-27.3	0,0730	0,0390	0,1180	0,0000
GK_KADA-2018-28.3	0,0730	0,0430	0,1460	0,0000
GK_KADA-2018-29.7	0,0690	0,0400	0,0740	0,0000
GK_KADA-2018-30.1	0,0690	0,0380	0,0780	0,0000
GK_KADA-2018-30.3	0,4250	0,1390	1,2610	0,7100
GK_KADA-2018-30.4	0,1570	0,0800	0,5210	0,2400
GK_KADA-2018-30.6	0,1570	0,1180	0,3070	0,3100
GK_KADA-2018-30.8	0,2200	0,0880	0,5260	0,4900
GK_KADA-2018-31.1	0,0800	0,0360	0,0800	0,0100
GK_KADA-2018-31.3	0,0850	0,0395	0,1390	0,0200
GK_KADA-2018-31.5	0,1200	0,0530	0,2810	0,1300
GK_KADA-2018-31.7	0,1680	0,0800	0,3260	0,2100
GK_KADA-2018-31.9	0,1550	0,1100	0,2800	0,2800
GK_KADA-2018-31.10	0,0950	0,0990	0,1390	0,0300

9.5 Metals in 40 mL of solution

After the AAS experiment, the mass of metals leached to 40 ml or 0,04 l of de-ionized water solution was calculated using the equation 13 from sub-section methodology 7.1. The highest value for Co, Li, Ni and Zn were found to be 0,0170, 0,0056, 0,0504 and 0,0284 milligrams respectively while the lowest were 0,0024, 0,0014, 0,0027 and 0 milligrams. . Blue and red color indications represent soil profile GK_KADA-2018-30 and GK_KADA-2018-31. The grey color represents the highest value in milligram while green color represents the lowest value. Co, Li, Ni and Zn represents cobalt, lithium, nickel and zinc respectively.

TABLE 18. The mass of several metals leached to 40 ml of water solution

Sample	Co leached mg	Li leached mg	Ni leached mg	Zn leached mg
GK_KADA-2018-20.4	0,0024	0,0019	0,0027	0
GK_KADA-2018-21.4	0,0025	0,0018	0,0043	0
GK_KADA-2018-22.6	0,0066	0,0020	0,0209	0,0048
GK_KADA-2018-23.5	0,0028	0,0014	0,0035	0
GK_KADA-2018-24.4	0,0064	0,0049	0,0170	0,0096
GK_KADA-2018-24.5	0,0064	0,0053	0,0140	0,0048
GK_KADA-2018-24.7	0,0042	0,0032	0,0077	0,0024
GK_KADA-2018-25.4	0,0028	0,0018	0,0112	0
GK_KADA-2018-26.3	0,0029	0,0016	0,0052	0
GK_KADA-2018-27.3	0,0029	0,0016	0,0047	0
GK_KADA-2018-28.3	0,0029	0,0017	0,0058	0
GK_KADA-2018-29.7	0,0028	0,0016	0,0030	0
GK_KADA-2018-30.1	0,0028	0,0015	0,0031	0
GK_KADA-2018-30.3	0,0170	0,0056	0,0504	0,0284
GK_KADA-2018-30.4	0,0063	0,0032	0,0208	0,0096
GK_KADA-2018-30.6	0,0063	0,0047	0,0123	0,0124
GK_KADA-2018-30.8	0,0088	0,0035	0,0210	0,0196
GK_KADA-2018-31.1	0,0032	0,0014	0,0032	0,0004
GK_KADA-2018-31.3	0,0034	0,0016	0,0056	0,0008
GK_KADA-2018-31.5	0,0048	0,0021	0,0112	0,0052
GK_KADA-2018-31.7	0,0067	0,0032	0,0130	0,0084
GK_KADA-2018-31.9	0,0062	0,0044	0,0112	0,0112
GK_KADA-2018-31.10	0,0038	0,0040	0,0056	0,0012

9.5.1 Metals leached from soil to water

The mass of the metals leached from soil to water represented by Table 18 was further divided by the mass of metals present in sample (table 13,14 ,15 and 16) to obtain the leached metal percentage from

soil to water using equation 14. The highest metal percentage leached for Co, Li, Ni and Zn were 93,2961%, 35,0493%, 81,9147% and 36,9406 % while the lowest were 5,2853 %, 1,9958%, 0,9426%and 0% respectively. Blue and red color indications represent soil profile GK_KADA-2018-30 and GK_KADA-2018-31. The grey color represents the highest value in percentage while green color represents the lowest value and red color X symbol represents the absence of value for further calculation. Co, Li, Ni and Zn represents Cobalt, Lithium, Nickel and Zinc respectively.

TABLE 19. Table metals percentage leached from soil to water.

Sample	Co leached %	Li leached %	Ni leached %	Zn leached %
GK_KADA-2018-20.4	5,2853	1,9958	2,5251	0,0000
GK_KADA-2018-21.4	21,1125	8,1515	5,7908	0,0000
GK_KADA-2018-22.6	18,8414	5,0398	15,4452	1,7511
GK_KADA-2018-23.5	11,9845	3,1894	4,3233	0,0000
GK_KADA-2018-24.4	40,9531	19,7868	23,8249	12,9277
GK_KADA-2018-24.5	10,3943	4,0524	10,0307	0,7912
GK_KADA-2018-24.7	11,2412	4,4100	8,5528	0,5498
GK_KADA-2018-25.4	15,0839	3,6779	9,8095	0,0000
GK_KADA-2018-26.3	33,4967	9,3699	8,5752	0,0000
GK_KADA-2018-27.3	27,0914	7,7934	5,2177	0,0000
GK_KADA-2018-28.3	14,2518	3,9176	0,9426	0,0000
GK_KADA-2018-29.7	34,5667	11,6353	11,5049	0,0000
GK_KADA-2018-30.1	X	X	X	X
GK_KADA-2018-30.3	93,2961	26,4145	81,9147	36,9406
GK_KADA-2018-30.4	73,6974	35,0493	36,2315	11,1348
GK_KADA-2018-30.6	48,7165	18,7540	23,5351	6,8477
GK_KADA-2018-30.8	31,8353	6,8173	30,7948	4,5180
GK_KADA-2018-31.1	X	X	X	X
GK_KADA-2018-31.3	69,5803	21,0173	18,0390	1,8196
GK_KADA-2018-31.5	76,0448	33,5865	28,0598	17,1560
GK_KADA-2018-31.7	54,8769	16,0811	22,2234	7,4214
GK_KADA-2018-31.9	50,0445	16,3917	19,3721	7,0144

Sample	Co leached %	Li leached %	Ni leached %	Zn leached %
GK_KADA-2018-31.10	10,1744	4,6925	5,9638	0,2540

10 CONCLUSIONS

The laboratory method presented in this thesis is used for the determination of the metals that are leached from Finnish AS soils to water as well as the metal content in samples taken from the field. Implementation of AAS methodology for cobalt, lithium, nickel and zinc were successfully completed. From the experimental results and discussion section, clear observation can be made between oxidized, transition and reduced zones. For soil profile GK-KADA-2018-30, the oxidized soil is located until 0.6 meters from top with a pH range of 3.9-3.7 while the reduced zone is located at depth below 0.8 meters with a pH range of 6.1 -6.9. On the other hand, for soil profile GK-KADA-2018-31, oxidized soil is located at until the depth of 1.2 meters from top with pH range of 3.6-4.8 while reduced zone is located at depth of 1.5 - 2 meters with a pH of 6.5 – 6.8. The differences in depth for the occurrence of oxidized and reduced layer can be observed (FIGURE 4) which depends upon the water level in these soils. The water level fluctuates throughout the year and facilitates the formation of AS soils. In the spring the water level is higher when snow melts and lower in summer in Finland. The average water level in these soils (sampling soils) is 1.2 meters. The details for the formation of oxidation and reduction mechanism can be found in sulfur redox chemistry and general principles section 3.

The metals in sample are present in high amount in bottom reduced soils while less in top oxidized soils. This is because, the oxidized soils are already oxidized and leached in the field while that of reduced soil are still available in sample for further oxidation or leaching. The metals amount present in soil profiles GK-KADA-2018- 30 and GK-KADA-2018- 31 are widely and narrowly distributed (from Figure 28 and 29). Zinc is abundant while cobalt is least available in both profiles soil samples. However, it is found that cobalt is leached excessively with 80,0619% while zinc is 0%. The metals are leached mostly from oxidized soils in both soil profiles while leached less from reduced soils. This can be explained from the composition of the soil which was not homogeneous. For example, soil profile GK-KADA-2018-31.3 is organically rich, GK-KADA-31.5 consists of fine sand and GK-KADA-31.10 is clay sand. The inconsistency in soil composition is the reason for least leaching of metals from reduced soils.

Finally, the AS soils are the oxidation product of PAS soils and are formed by postglacial land uplift and anthropogenic activities. AS soils facilitates metals leaching of metals due to the dissolution of minerals from AS soils to water bodies and affects the aquatic life, vegetation, infrastructure and human beings

in several ways. Therefore, it is necessary to make serious efforts to develop methods such as implementation of Control Subsurface Drainage and Control Subsurface Irrigation for prevention of contamination.

REFERENCES

Abate E, Hussien S, Laing M, Mengistu F. Aluminium toxicity tolerance in cereals: Mechanisms, genetic control and breeding methods. African Journal of Agricultural Research. 2013;8(9):711–722

Albretsen, J. 2006. The toxicity of iron, an essential element. Veterinary medicine-bonner springs then edwardsville 101(2), 82.

Alhonen, P., Mantere-Alhonen, S., & Vuorinen, A. 1997. Preliminary observations on the metal content in some milk samples from an acid geoenvironment. Bulletin-geological society of Finland, 69, 31-41.

Arnio, B. 1928. Agrogeologiska kartor N:o 5. Syd-Österbotten. Statens Markforskningsinstitut. 80

Adriesse, W., van Mensvoort, M. 2006. Acid sulfate soil: distribution and extent. Encyclopedia of soil science 1, 14-19.

Aoshima, K. 2016. itai-itai disease: Rental tubular osteomalacia induced by environmental exposure to cadmium-historical review and perspectives. Soil Science and Plant Nutrition 62(4), 319-326.

Arkesteyn, G. J. M. W. 1980. Pyrite oxidation in acid sulphate soils: The role of miroorganisms. Plant and Soil, 54(1), 119-134.

Baby, J., Raj, J. S., Biby, E. T., Sankarganesh, P., Jeevitha, M. V., Ajisha, S.
U., & Rajan, S. S. 2010. Toxic effect of heavy metals on aquatic environments. International journal of biological and chemical sciences 4(4), 939-952.

Baldisserotto, B., Kamunde, C., Matsuo, A., & Wood, C. M. 2004. A protective effect of dietary calcium against acute waterborne cadmium uptake in rainbow trout. Aquatic Toxicology, 67(1), 57-73.

Barbara, J. & Malgorzata, W. 2006. The metal uptake and accumulation in fish living in polluted waters. Soil and Water Pollution Monitoring Protection and Remediation, 107-114.

Bentley, P. J. 1991. A high-affinity zinc-binding plasma protein in channel catfish (Ictalurus punctatus). Comparative Biochemistry and Physiology Part C: Comparative Pharmacology, 100(3), 491-494.

Berner, R.A. 1984. Sedimentary pyrite formation: An update. Geochimica et Cosmochimica Acta 48, 605-615.

Biswas, S., Prabhu, R. K., Hussain, K. J., Selvanayagam, M., & Satpathy, K. K. 2012. Heavy metals concentration in edible fishes from coastal region of Kalpakkam, southeastern part of India. Environmental monitoring and assessment, 184(8), 5097-5104.

Bloomfield, C. 1972. Acidification and ochre formation in pyritic soils. In Proceedings of the International Symposium on Acid Sulphate Soils, 13-20.

Boman, A. 2008. Sulphur dynamics in boreal potential and actual acid sulphate soils rich in metastable iron sulphide. Åbo Akademy University Press. Doctoral Dissertation.

Boman, A., Becher, M., Mattbäck, S., Sohlenius, G., Auri, J., Öhrling, C., Liwata-Kenttälä, P. & Edén, P. 2019. Classification of acid sulfate soils in Finland and Sweden.

Boman, A., Åström, M., & Fröjdö, S. 2008. Sulfur dynamics in boreal acid sulfate soils rich in metastable iron sulfide-the role of artificial drainage. Chemical Geology 255(1-2), 68-77.

Boman, A., Fröjdö, S., Backlund, K., & Åström, M. E. 2010. Impact of isostatic land uplift and artificial drainage on oxidation of brackish-water sediments rich in metastable iron sulfide. Geochimica et Cosmochimica Acta 74(4), 1268-1281.

Breemen, N. V. 1973. Soil forming processes in acid sulphate soils. Proceedings of the international Symposium on Acid Sulphate Soils, 13-20 August 1972. Wageningen, the Netherlands: ILRI publication18, 66-130.

Breemen, N. V. 1982. Genesis, Morphology, and Classification of Acid Sulfate Soils in Coastal Plains 1. Acid sulfate weathering, 95-108.

Burton, E. D., Bush, R. T., & Sullivan, L. A. 2006. Sedimentary iron geochemistry in acidic waterways associated with coastal lowland acid sulfate soils. Geochimica et Cosmochimica Acta, 70(22), 5455-5468.

Burton, E. D., Bush, R. T., Sullivan, L. A., & Mitchell, D. R. 2007. Reductive transformation of iron and sulfur in schwertmannite-rich accumulations associated with acidified coastal lowlands. Geochimica et Cosmochimica Acta, 71(18), 4456-4473.

Butler, I. B., Böttcher, M. E., Rickard, D., & Oldroyd, A. 2004. Sulfur isotope partitioning during experimental formation of pyrite via the polysulfide and hydrogen sulfide pathways: implications for the interpretation of sedimentary and hydrothermal pyrite isotope records. Earth and Planetary Science Letters, 228(3-4), 495-509.

Böttcher, M. E., Smock, A. M., & Cypionka, H. 1998. Sulfur isotope fractionation during experimental precipitation of iron (II) and manganese (II) sulfide at room temperature. Chemical Geology, 146(3-4), 127-134.

Clayton, B.00201989. Water pollution at Lowermoor, North Cornwall. Report of the Lowermoor Incident Health Advisory Group, Cornwall and Isles of Scilly District Health Authority, Truro, Cornwall.

Crist, R. H., Oberholser, K., Schwartz, D., Marzoff, J., Ryder, D., & Crist, D. R. 1988. Interactions of metals and protons with algae. Environmental science & technology, 22(7), 755-760.

Çoğun, H. Y., & Kargın, F. 2004. Effects of pH on the mortality and accumulation of copper in tissues of Oreochromis niloticus. Chemosphere, 55(2), 277-282.

Datta. S. 2019. A brief note on iron deficiency in plants and its correction. Indian council of Agricultural Research, Kolkata. Available: https://www.researchgate.net/publication/330133913_A_brief_Note_on_Iron_Deficiency_in_Plants_and_its_Correction. Accessed. 6th December 2019.

Dent, D. L. 1986. Acid sulphate soils: a baseline for research and development (No. 39). ILRI-publication 39. Wageningen, The Netherlands. 204.

Dent, D. L., & Pons, L. J. 1995. A world perspective on acid sulphate soils. Geoderma 67(3-4), 263-276.

Erviö, R., & Palko, J. 1984. Macronutrient and micronutrient status of cultivated acid sulphate soils at Tupos, Finland. Ann. Agric. Fenn (23), 121–134.

Evangelou, V. P., & Zhang, Y. L. 1995. A review: pyrite oxidation mechanisms and acid mine drainage prevention. Critical Reviews in Environmental Science and Technology, 25(2), 141-199.

Fatima, M., & Usmani, N. 2013. Histopathology and bioaccumulation of heavy metals (Cr, Ni and Pb) in fish (Channa striatus and Heteropneustes fossilis) tissue: A study for toxicity and ecological impacts. Pakistan J biol Sci, 16, 412-420.

Fältmarsch, R. M., Åström, M. E., & Vuori, K. M. 2008. Elemental risks of metals mobilised from acid sulphate soils in Finland: a literature review. Boreal Environmental Research 13, 444-456.

Fältmarsch, R. 2010. Biogeochemistry in acid sulphate soil landscapes and small urban centers in Western Finland. Åbo Akademy University. Ph.D thesis.

Gorell, J. M., & Checkoway, H. 2001. Epidemiological Studies: Risk Factors-Session IV Summary and Research Needs. Neurotoxicology, 6(22), 837-844.

Gorell, J. M., Johnson, C. C., Rybicki, B. A., Peterson, E. L., Kortsha, G. X., Brown, G. G., & Richardson, R. J. 1997. Occupational exposures to metals as risk factors for Parkinson's disease. Neurology, 48(3), 650-658.

Gorell, J. M., Johnson, C. C., Rybicki, B. A., Peterson, E. L., & Richardson, R. J. 1998. The risk of Parkinson's disease with exposure to pesticides, farming, well water, and rural living. Neurology, 50(5), 1346-1350.

Gorell, J. M., Johnson, C. C., Rybicki, B. A., Peterson, E. L., Kortsha, G. X., Brown, G. G., & Richardson, R. J. 1999. Occupational exposure to manganese, copper, lead, iron, mercury and zinc and the risk of Parkinson's disease. Neurotoxicology, 20(2-3), 239-247.

Government of Western Australia. 2014. Soil pH and plant health. Available: https://www.agric.wa.gov.au/soil-ph-and-plant-health?. Accessed 28 February 2019.

Government of western Australia. 2015. What are acid sulfate soils? Available:https://www.der.wa.gov.au/your-environment/acid-sulfate-soils/64acid-sulfate-soils-in-wa. Accessed 28 February 2019.

Government of Western Australia. 2019. Waterlogging: the science. https://www.agric.wa.gov.au/waterlogging/waterlogging-science?page=0%2C0#smartpaging_toc_p0_s0_h2.

Grieb, T. M., Bowie, G. L., Driscoll, C. T., Gloss, S. P., Schofield, C. L., & Porcella, D. B. 1990. Factors affecting mercury accumulation in fish in the upper Michigan peninsula. Environmental Toxicology and Chemistry: An International Journal, 9(7), 919-930.

Gupta, N., Gaurav, S. S., & Kumar, A. 2013. Molecular basis of aluminium toxicity in plants: a review. American Journal of Plant Sciences, 4(12), 21.

Guterres, J., Rossato, L., Doley, D., & Pudmenzky, A. 2018. A new conceptual framework for plant responses to soil metals based on metal transporter kinetic parameters. Journal of Hazardous Materials, 449-467.

Hart, M. G. R. 1962. Observations on the source of acid in empoldered mangrove soils. Plant and Soil, 17(1), 87-98.

Jaishankar, M., Tseten, T., Anbalagan, N., Mathew, B. B., & Beeregowda, K. N. 2014. Toxicity, mechanism and health effects of some heavy metals. Interdisciplinary Toxicology 7(2), 60-72.

Jezierska, B., Ługowska, K., & Witeska, M. 2009. The effects of heavy metals on embryonic development of fish (a review). Fish physiology and biochemistry, 35(4), 625-640.

Jezierska, B., & Witeska, M. 2006. The metal uptake and accumulation in fish living in polluted waters. In Soil and water pollution monitoring, protection and remediation. Springer, Dordrecht, 107-114.

Järup, L. 2003. Hazards of heavy metal contamination. British medical bulletin 68(1),167-182.

Karimian, N., Johnston, S. G., & Burton, E. D. 2018. Iron and sulphur cycling in acid sulfate soil wetlands under dynamic redox conditions: A review. Chemosphere 197. 803-816.

Katyal, A., & Morrison, R. D. 2007. Forensic applications of contaminant transport models in the subsurface. In Introduction to Environmental forensics (eds.) 2nd edition. Burlington, San Diego, London: Elsevier Academic Press, 513-575. (ScienceDirect, topic: Hydrolysis. Academic Press.

Klu. B.A. 2017. Mitigating the Release of acidity and metals from an acid Sulphate Soil: A study using column experiment. Novia University of Applied Sciences. Bacheor's thesis.

Lahermo P., Väänänen P., Tarvainen T. & Salminen R. 1996. Geochemical atlas of Finland, Part 3: Environmental geochemistry — stream waters and sediments. Geological Survey of Finland, Espoo.

Ljung, K., Maley, F., Cook, A., & Weinstein, P. 2009. Acid sulfate soils and human health - a millennium ecosystem assessment. Environment International 35(8), 1234-1242.

Luther III, G. W. 1991. Pyrite synthesis via polysulfide compounds. Geochimica et Cosmochimica Acta, 55(10), 2839-2849.

Mattbäck, S., Boman, A., & Österholm, P. 2017. Hydrogeochemical impact of coarse-grained post-glacial acid sulphate soil materials. Geoderma 308, 291-301.

Mokma, D. L., Yli-Halla, M., & Hartikainen, H. 2000. Soils in a young landscape on the coast of southern Finland. Agricultural and Food Science, *9*(4), 291-302.

Morse, J. W., & Rickard, D. 2004. Chemical Dynamics of Sedimentary Acid Volatile Sulfide. Environmental Science & Technology A-pages 38, 131A-136A.

National Board of Waters. 1973. Selvitys Kyrönjoen ja sen edustan merialueen kalakuolemien syistä. 101.

Nordmyr, L., Boman, A., Åström, M., & Österholm, P. 2006. Estimation of leakage of chemical elements from boreal acid sulphate soils. Boreal Environment Research 11, 261-273.

Nordstrom, D. K. 1982. Aqueous pyrite oxidation and the consequent formation of secondary iron minerals. Soil Science Society of America, 37-56.

Nystrand, M. I., Österholm, P., Yu, C., & Åström, M. 2016. Distribution and speciation of metals,phosphorous, sulfate and organic material in brackish estuary water affected by acid sulphate soils. Applied Geochemistry 66, 264-279.

Nesbitt, B. 2007. Handbook of valves and actuators: valves manual international. Elsevier, 56.

Palko, J. 1986. Mineral element content of Timothy (Phleum pratense L.) in an acid sulphate soil area of Tupos Village, Northern Finland. Acta Agriculturae Scandinavica, 36(4), 399-409.

Palko, J .1994. Acid sulphate soil and their agricultural and environmental problems in Finland. PhD thesis, University of Oulu, Finland.58.

Palko J. & Yli-Halla M. 1988. Solubility of Co, Ni and Mn in some extractants in a Finnish acid sulphate soil area. Acta Agric. Scand. 38: 153–158.

Pandey, G., & Madhuri, S. 2014. Heavy metals causing toxicity in animals and fishes. Research journal of Animal, Veterinary and Fishery science 2(2), 17-23.

Prasad, J., Jain, D. K., & Ahuja, A. K. 2006. Factors influencing the sulphate resistance of cement concrete and mortar. Asian Journal of Civil Engineering 7(3), 259-268.

Price, F. T., & Shieh, Y. N. 1979. Fractionation of sulfur isotopes during laboratory synthesis of pyrite at low temperatures. Chemical Geology, 27(3), 245-253.

Purokoski, P. 1958. Die Schwefelhaltigen Tonsedimente in Dem Flachlandgebiet Von Liminka Im Lichte Chemischer Forschung. Agrogeologisia Julkaisuja 70, 1-88.

Puurokoski, P. 1959. Rannikoseudun rikkipitoista maista. Agrogeologisia Julkaisia 74. 1-23.

Rickard, D. 1995. Kinetics of FeS precipitation: Part 1. Competing reaction mechanisms. Geochimica et Cosmochimica Acta, 59(21), 4367-4379.

Queensland Government. 2013. Identifying acid sulfate soil. Available: https://www.qld.gov.au/environment/land/management/soil/acid-sulfate/identified. Accessed 28 February 2019.

Rickard, D. 1997. Kinetics of pyrite formation by the H2S oxidation of iron (II) monosulfide in aqueous solutions between 25 and 125 C: the rate equation. Geochimica et Cosmochimica Acta, 61(1), 115-134.

Rickard, D., & Luther, G. W. 2007. Chemistry of iron sulfides. Chemical reviews, 107(2), 514-562.

Rickard, D., & Morse, J. W. 2005. Acid volatile sulfide (AVS). Marine chemistry, 97(3-4), 141-197.

Rickard, D., & Luther III, G. W. 1997. Kinetics of pyrite formation by the H2S oxidation of iron (II) monosulfide in aqueous solutions between 25 and 125 C: the mechanism. Geochimica et Cosmochimica Acta, 61(1), 135-147.

Rickard, D., Griffith, A., Oldroyd, A., Butler, I. B., Lopez-Capel, E., Manning, D. A. C., & Apperley, D. C. 2006. The composition of nanoparticulate mackinawite, tetragonal iron (II) monosulfide. Chemical Geology, 235(3-4), 286-298.

Roos M. & Åström M. 2005. Hydrogeochemistry of rivers in an acid sulphate soil hotspot area in western Finland. Agric. Food Sci. 14: 24–33.

Schludermann, C., Konecny, R., Laimgruber, S., Lewis, J. W., Schiemer, F., Chovanec, A., & Sures, B. 2003. Fish macroparasites as indicators of heavy metal pollution in river sites in Austria. Parasitology, 126(7), S61-S69.

Spicer, J. I., & Weber, R. E. 1991. Respiratory impairment in crustaceans and molluscs due to exposure to heavy metals. Comparative biochemistry and physiology. C, Comparative pharmacology and toxicology, 100(3), 339-342.

Starkey, R. L. 1966. Oxidation and reduction of sulfur compounds in soils. Soil Science, 101(4), 297-306.

Steffen, H., & Kaufmann, G. 2005. Glacial isostatic adjustment of Scandinavia and northwestern Europe and the radial viscosity structure of the Earth's mantle. Geophysical Journal International 163(2), 801-812.

Schippers, A., & Jørgensen, B. B. 2001. Oxidation of pyrite and iron sulfide by manganese dioxide in marine sediments. Geochimica et Cosmochimica Acta, 65(6), 915-922.

Schippers, A., & Jørgensen, B. B. 2002. Biogeochemistry of pyrite and iron sulfide oxidation in marine sediments. Geochimica et Cosmochimica Acta, 66(1), 85-92.

Sohlenius, G., & Öborn, I. 2004. Geochemistry and partitioning of trace metals in acid sulphate soils in Sweden and Finland before and after sulphide oxidation. Geoderma, 122(2-4), 167-175.

Sundström, R., Åström, M., & österholm, P. 2002.Comparison of the metal content in acid sulfates oil run off and industrial effluents in Finland. Environmental science & technology 36(20), 4269-4272.

Sullivan, L. A., & Bush, R. T. 2004. Iron precipitate accumulations associated with waterways in drained coastal acid sulfate landscapes of eastern Australia. Marine and Freshwater research, 55(7), 727-736.

Toivonen, J., Österholm, P., & Fröjdö, S. 2013. Hydrological Processes behind annual and decadal - scale variations in the water quality of runoff in Finnish catchments with acid sulphate soils. Journal of hydrology 487, 60-69.

U.S EPA (Environmental Protection Agency). 2011. A Field-based aquatic life benchmark for conductivity in central appalachian streams. Office of research and development, National center for environmental assessment, Washington, DC, EPA/600/R-10/023F.

Uusi-Kämppä, J., Keskinen, R., Heikkinen, J., Guagliardi, I., &Nuutinen, V.2019. A map-based comaprison of chemical characteristics in the surface horizon of acid and non-acid sulfate soils in coastal areas of Finland. Journal of Geochemical Exploration 200, 193-200.

Understanding cement. 2005. Available: http://understandingcement.com/. Accessed 22 March 2019.

Virtanen, S., Simojoki, A., Rita, H., Toivonen, J., Hartikainen, H., & Yli-Halla, M. 2014. A multi-scale comparison of dissolved Al, Fe, and S in boreal acid sulphate soil. Science of the Total Environment 499, 336-348.

Wang, H., Liang, Y., Li, S., & Chang, J. 2013. Acute toxicity, respiratory reaction, and sensitivity of three cyprinid fish species caused by exposure to four heavy metals. PloS one, 8(6), e65282.

Wang, Q., & Morse, J. W. 1996. Pyrite formation under conditions approximating those in anoxic sediments I. Pathway and morphology. Marine Chemistry, 52(2), 99-121.

Wessel, B. M., Fiola, J. C., & Rabenhorst, M. C. 2017. Soil morphology, genesis and monolith construction of an acid sulphate soil with silica-cementation in the US Mid-Atlantic Region. Geoderma 308, 260-269.

Ward, N. J., Sullivan, L. A., Fyfe, D. M., Bush, R. T., & Ferguson, A. J. 2004. The process of sulfide oxidation in some acid sulfate soil materials. Soil Research, 42(4), 449-458.

Wikilander, L., Halloren, G., & Jonsson, E. 1950. Studies on gyttja soils, III. Rate of sulfur oxidation. Kungliga Lantbrukshogskolans Annaler, 17, 425-440.

Wolthers, M., Van der Gaast, S. J., & Rickard, D. 2003. The structure of disordered mackinawite. American Mineralogist, 88(11-12), 2007-2015.

Yamazaki, M., Tanizaki, Y., & Shimokawa, T. 1996. Silver and other trace elements in a freshwater fish, Carasius auratus langsdorfii, from the Asakawa River in Tokyo, Japan. Environmental Pollution, 94(1), 83-90.

Yli-Halla, M. 1997. Classification of acid sulphate soils of Finland according to Soil Taxonomy and the FAO/Unesco legend. Agricultural and Food Science, 6(3), 247-258.

Yli-Halla, M., & Palko, J. 1987. Mineral element content of oats (Avena sativa L.) in an acid sulphate soil area of Tupos village, northern Finland. Agricultural and Food Science, 59(2), 73-78.

Yli-Halla, M., Virtanen, S., Mäkelä, M., Simojoki, A., Hirvi, M., Innanen, S., Mäkelä, J.J., & Sullivan, L. 2017. Abudant stocks and mobilization of elements in boreal acid sulfate soils. Geoderma 308. 333-340.

Yli-Halla, M, Puustinen, M. & koskiaho,J. 1999.Area of cultivated acid sulphate soils in Finland. Soil use and Management 15, 62-67.

Zeitoun, M. M., & Mehana, E. E. 2014. Impact of water pollution with heavy metals on fish health: Overview and Updates. Global Veterinaria 12(2), 219-231.

Zhou, T., Weis, P., & Weis, J. S. 1998. Mercury burden in two populations of Fundulus heteroclitus after sublethal methylmercury exposure. Aquatic Toxicology, 42(1), 37-47.

Åström, M. 1998. Mobility of Al, P and alkali and alkaline earth metals in acid sulphate soils in Finland. Science of the total environment, 215(1-2), 19-30.

Åström M. 2001a. The effect of acid soil leaching on trace element abundance in a medium-sized stream, W. Finland. Applied Geochemistry, 16: 387–396.

Åström M. 2001b. Effect of widespread severely acidic soils on spatial features and abundance of trace elements in streams. Journal of Geochemical Exploration, 73 (3) 181–191.

Åström, M., & Åström, J. 1997. Geochemistry of stream water in a catchment in Finland affected by sulphidic fine sediments. Applied Geochemistry, 12(5), 593-605.

Åström, M., & Björklund, A. 1995. Impact of acid sulphate soils on stream water geochemistry in western Finland. Journal of Geochemical Exploration 55(1-3), 163-170.

Åström M. & Björklund A. 1996. Hydrogeochemistry of a stream draining sulfide-bearing postglacial sediments in Finland. Water Air and Soil Pollution, 89 (3-4), 233–246.

Åström, M., & Björklund, A. 1997. Geochemistry and acidity of sulphide-bearing postglacial sediments of western Finland. Environmental Geochemistry and Health, 19(4), 155-164.

Åström M. & Corin N. 2000. Abundance, sources and speciation of trace elements in humus-rich streams affected by acid sulphate soils. Aquatic Geochemistry 6(3), 367–383.

Österholm P. 2005. Previous, current and future leaching of sulphur and metals from acid sulphate soils in W. Finland. Ph.D. thesis, Åbo Akademi Univeristy, Turku, Finland

Österholm, P., & Åström, M. 2002. Spatial trends and losses of major and trace elements in agricultural acid sulphate soils distributed in artificially drained Rintala area,W.Finland. Applied Geochemistry 17(9), 1209-1218.

Österholm, P., Virtanen, S., Rosendahl, R., Uusi-Kämppä, J., Ylivainio, K., YliHalla, M., Mäensivu, M., & Turtola, E. 2015. Groundwater management of acid sulfate soils using controlled drainage, by-pass flow prevention, and subsurface irrigation on a boreal farmland. Acta Agriculturae Scandinavica, Section B—Soil & Plant Science, 65(sup1), 110-12.